RUSSIAN JOURNAL OF EARTH SCIENCES, VOL. 4, NO. 2, PAGES 121–151, APRIL 2002

# Petrology and geochemistry of rocks from the basement of the Pechenga paleorift

V. R. Vetrin [1], O. M. Turkina [2], and J. Ludden [3]

[1] Geological Institute, Kola Science Centre, Russian Academy of Sciences, Apatity, Murmanskaya oblast, 184209 Russia
[2] United Institute of Geology, Geophysics, and Mineralogy, Siberian Branch of Russian Academy of Sciences, Novosibirsk, 630090 Russia
[3] Centre for Petrographic and Geochemical Researches, Nancy (CRPG-CNRS), France

**Abstract.** The basement of the Early Proterozoic Pechenga paleorift was penetrated by the Kola Superdeep Borehole over a depth interval of 6842–12,261 m. The principal types of basement rocks are gneisses of trondhjemite–tonalite composition in association with amphibolites, gneisses containing aluminous minerals, and banded iron formation (BIF). It was demonstrated that the paleorift basement and rock associations exposed at the surface in the northwestern part of the Kola–Norwegian block are of similar age, composition of their protoliths, and correspond to the main types of sedimentary–volcanic and plutonic rocks of the Archean granite–greenstone terrane, which was broken up into separate segments in the Early Proterozoic. Rocks of the Pechenga Archean basement were affected by Proterozoic magmatism and metasomatism related to the rift development. The most intense Proterozoic processes in the Pechenga basement and its nearest surroundings were intrusion of numerous mafic–ultramafic bodies, retrograde metamorphism to the medium–low-temperature amphibolite and epidote amphibolite facies, synmetamorphic migmatization, and emplacement of postkinematic granite dikes. Most Proterozoic processes were determined to have been related to mantle sources. The overall amounts of Proterozoic material introduced into the Archean rocks penetrated by the lowermost part of the borehole plus the remobilized Archean crustal material were estimated at ≥30% (≥12–15% amphibolites, ∼3% granite veins, and ∼15% migmatized rocks).

## Introduction

The early history of the Earth is one of the most interesting problems of modern geology. The pivotal point of this problem is the nature of the primary crust in various areas, its composition, age, and genesis. An area convenient for studying these problems is the northeastern part of the Baltic Shield and, within this area, the Pechenga mining district, which is composed of Proterozoic sedimentary–volcanic rocks and Archean amphibolite–gneiss complexes. These were penetrated by the Kola Superdeep Borehole to a depth of 12,261 m. The geoblock hosts large Cu–Ni sulfide deposits, is exposed well enough at the surface, and was thoroughly examined by a variety of geological and geophysical techniques.

To a depth of 6842 m, the Kola Superdeep Borehole (KSDB) intersected the Early Proterozoic Pechenga sedimentary–volcanic complex and farther, up to the hole bottom, was drilled in the Archean metamorphic rocks of the basement of the Pechenga riftogenic structure. The geology, origin succession, age, and composition of Precambrian rocks from the KSDB section itself and from its closest surroundings were described in numerous papers and monographs [*Archean Complex...,* 1991; *Kola Superdeep Borehole,* 1984,



Paper number TJE02085.
ISSN: 1681–1208 (online)

The online version of this paper was published 16 April 2002.
URL: http://rjes.wdcb.ru/v04/TJE02085/TJE02085.htm

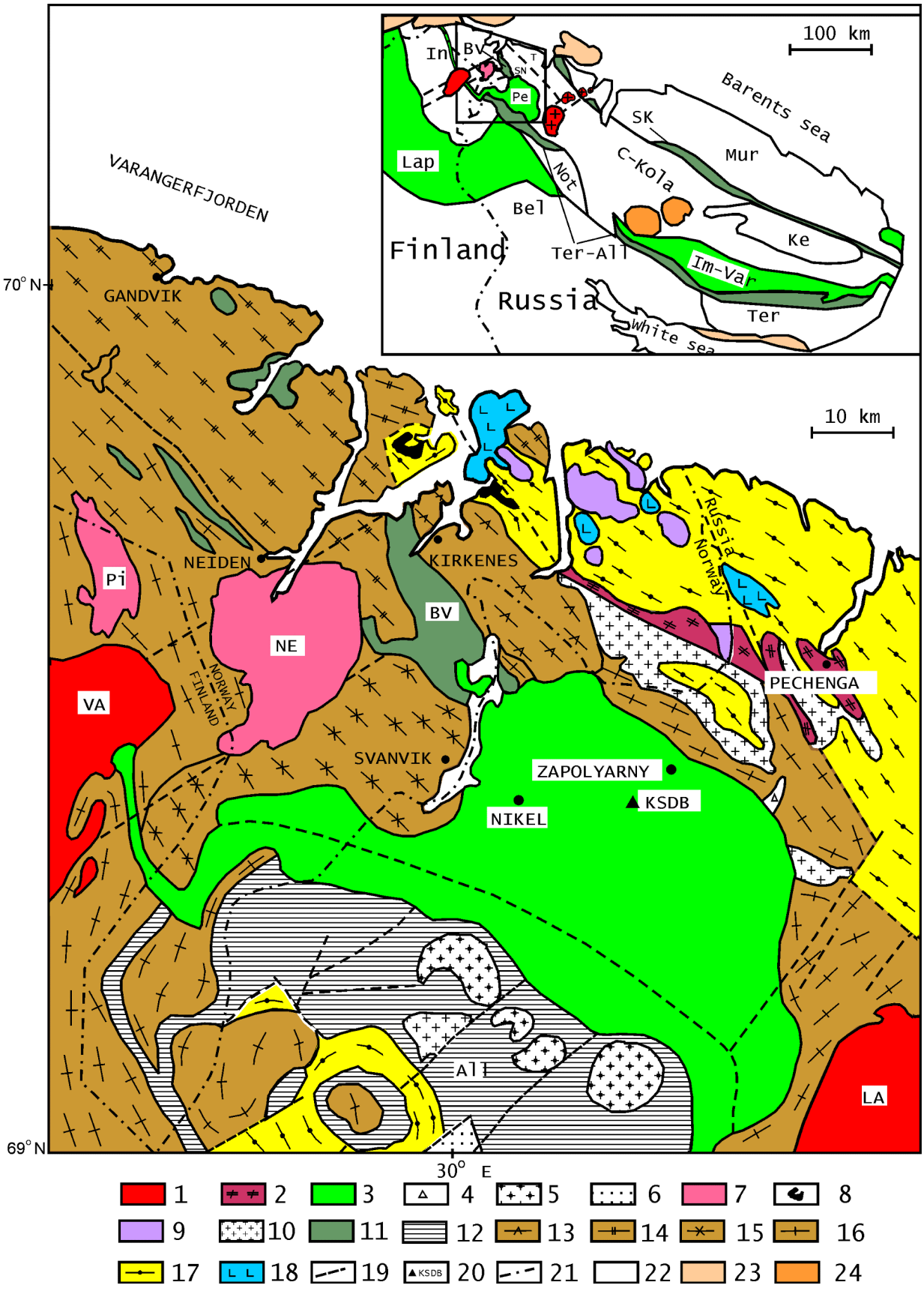
100 km
In
BV
T
SN
Pe
Lap
Not
Bel
Finland
Ter-All
Russia
SK
Barents sea
Mur
C-Kola
Ke
Im-Var
Ter
White sea
VARANGERFJORDEN
70° N
GANDVIK
10 km
Pi
NEIDEN
KIRKENES
BV
NE
VA
NORWAY
FINLAND
Russia
Norway
PECHENGA
SVANVIK
ZAPOLYARNY
KSDB
NIKEL
All
LA
69° N
30° E
1 2 3 4 5 6 7 8
9 10 11 12 13 14 15 16
17 18 19 20 21 22 23 24
KSDB

1998; *Kremenetsky and Ovchinnikov,* 1986; *Magmatic...,* 1986; and others]. The Pechenga Complex was studied particularly extensively, which made it possible to conduct a layer-by-layer correlation between rocks from the KSDB section and their surface analogues. The correlation and petrology of the Archean rocks are not as obvious because of their extensive folding, polycyclic metamorphism, and migmatization. There is still no consensus as to which rocks are analogues of the Archean complex of KSDB, whether these are the high-grade gneisses of the Kola Group exposed north and northeast of the Pechenga structure or the complexes of the Late Archean granite–greenstone terrane east and northwest of it. Only scanty information was obtained on the transformation processes of the Archean basement rocks in the course of the Early Proterozoic rifting, a process that was responsible for the intense reheating of the Archean rocks and their intrusion by vast masses of mantle material.

We carried out a geological and petrological–geochemical study of the principal types of Archean rocks from KSDB and from the framing of the Pechenga structure. The precise geochemical data obtained allowed us to reconstruct the composition of the protoliths. Much attention was paid thereby to the geochemistry of REE and some major, minor, and trace elements (Al, Mg, Ti, V, Th, Zr, Hf, Ta, Nb, Y, and others), which are the least mobile during regional metamorphism and metasomatism. We revealed the importance of the REE composition of the tonalite–trondhjemite gneisses for the correlation of Precambrian rock sequences. Rocks of the KSDB Archean complex were demonstrated to be similar to rocks of the Archean granite–greenstone terrane, and the Archean basement rocks were determined to have been significantly affected by processes related to the origin of the Early Proterozoic Pechenga paleorift.

## Geological Overview

The Kola Superdeep Borehole, which reached a record depths of 12,261 m, was drilled in the northern portion of the Pechenga structure in the northwestern part of the Murmansk district area, which is situated in the Kola subprovince of the Baltic Shield and includes the Kola Peninsula, part of northern Karelia, Finnish Lapland, and the Finnmark area in northern Norway. The subprovince consists of large crustal blocks (Murmansk, Kola–Norwegian, Inari, Notozero, Keivy, Belomorian, and Tersk), separated by Archean and Early Proterozoic mobile belts (Northern Kola, [*Smolkin et al.,* 2000]; Tersk–Allarechka, Pechenga–Imandra–Varzuga, and Lapland–Kolvitsa; Figure 1).

The 2.3- to 1.8-Ga Pechenga structure is part of an Early Proterozoic continental rift zone, which crosses the Kola Peninsula and consists of two major parts (Imandra–Varzuga and Pechenga) and a number of smaller local structures (Polmak, Pasvik, Keulik–Kenirim, and Ust' Ponoi). The origin and further evolution of the zone were controlled by the extension of the Archean basement and the development of its dome-shaped uplift, subsequent folding, subsidence, and a final folding episode during the orogenic stage [*Kola Superdeep Borehole,* 1998; *Smolkin et al.,* 1995; *Zagorodnyi et al.,* 1982]. It is believed that, during the development of the rift zone, its western and eastern flanks were partly juxtaposed with the Late Archean Tersk–Allarechka greenstone belt (Olenegorsk belt; [*Dobrzhinetskaya et al.,* 1995]), and, thus, this structure is "embedded".

The Poritash fault divides the Pechenga rift structure into the Northern and the Southern tectono–stratigraphic subzones, which differ in the compositions of their rocks and the styles of tectonic deformations. The southern margin of

**Figure 1.** Schematic geological map of northern Norway and the northwestern Kola Peninsula (prepared with the use of materials compiled from [*Dobrzhinetskaya et al.,* 1995; *Juve et al.,* 1995; *Kremenetsky and Ovchinnikov,* 1986]).
(1–6) Early Proterozoic rocks: (1) postkinematic granites and pegmatites (LA = the Litza–Araguba Complex, BA = Vainospaa Massif), (2) muscovite–microcline granites and migmatized rocks; (3) volcanosedimentary rocks of the Pechenga–Imandra–Varzuga belt; (4) mafic rocks; (5) tonalites and granodiorites; (6) granulites; (7–18) Late Archean rocks: (7) porphyritic granites (Pi = the Pirivaara Massif, NE = Neiden Massif), (8) quartz syenites and syenites, (9) monzonites and granodiorites, (10) plagioclase–microcline granites, (11) volcano-sedimentary rocks of greenstone belts, (12) undifferentiated rocks of the Tersk–Allarechka greenstone belt and the basement, (13–16) tonalite–trondhjemite–granodiorite rocks of different complexes: (13) Kirkenes, (14) Varanger, (15) Svanvik, (16) Garsjø, (17) gneisses with HAM, (18) enderbites; (19) projections of faults; (20) Kola Superdeep Borehole; (21) state boundaries.
The inset presents a schematic map of he tectonic zoning of the Kola subprovince of the Baltic Shield. (22) Archean rocks; (23) Late Proterozoic sedimentary rocks; (24) Paleozoic nepheline syenite intrusions. Blocks of Archean basement rocks: Mur = Murmansk, Ko-Nor = Kola–Norwegian (segments: T = Titovsky, SN = Svanvik–Neiden), Ke = Keivy, Ter = Tersk, In = Inari, Not = Notozero, Bel = Belomorian. Late Archean greenstone belts: NK = northern Kola, Ter–All = Tersk–Allarechka, Bv = Bjornevatn, Val = Valen. Early Proterozoic foldbelts: Pe-Im-Var = Pechenga–Imandra–Varzuga (paleoriftogenic structures: Pe = Pechenga, Im-Var = Imandra–Varzuga), Lap = Lapland granulite.

the Southern Pechenga subzone nearly everywhere occurs in contact with the Tersk–Allarechka greenstone belt, and only its western part is bounded by the granite–greenstone rock assemblages of the Inari block. The rocks of the Northern Pechenga subzone, where the Kola Superdeep Borehole was drilled, were combined into two series: Nikel and underlying Luostari, each of which is further subdivided into two volcanogenic suites, alternating with initially sedimentary lithologies. The volcanic evolution is reflected in the systematic compositional variations of the rocks from basaltic andesites and trachyandesitic basalts (Luostari suite) to tholeiitic basalts and ferropicrite–basalts (Nikel suite). The intrusions are sheet-shaped gabbro-diabase bodies, massifs of mafic and ultramafic rocks, and hypabyssal intrusions of andesite porphyry. The metamorphic grades of the rocks vary from the prehnite–pumpellyite facies to the lower and middle grades of the amphibolite facies, with the metamorphic grade increasing from upper to lower stratigraphic units [*Kola Superdeep Borehole,* 1984]. The Northern Pechenga subzone is hosted by gneiss-amphibolitic complexes of the Kola–Norwegian block (an Early Proterozoic composite terrane [*Balaganskii et al.,* 1998]), whose northwestern termination is made up of the Svanvik–Neiden and Titovsky Archean segments.

The southwestern boundary between the Svanvik–Neiden terrane and the Inari block is drawn along a system of faults, which controlled the position of the Early Proterozoic Polmak–Pasvik–Pechenga structures. In the east, it is bounded by a northeast-trending deep fault, which is marked by granite porphyry intrusions of the Litza–Araguba Complex [*Vetrin et al.,* 1975]. The northern boundary with the Titovsky segment is also tectonic; it served as the conduit for the Kirkenes tonalite–trondhjemite pluton (dated at 2.8 Ga; [*Levchenkov et al.,* 1995]) and is marked by the development of a diversity of anatectic granites and migmatized rocks, dated at 2.8–2.15 Ga [*Ts'on' et al.,* 1988; *Vinogradov,* 1978]. The predominant supracrustal associations of this segment are Archean tonalite–trondhjemite complexes (∼80–90%) with scattered relics of greenstone structures, the largest of which is the Bjørnevatn greenstone structure, consisting of micaceous gneisses, schists, amphibolites, and BIF [*Siedleska et al.,* 1985]. The U–Pb zircon age of the tonalite–trondhjemite gneisses was estimated at 2.8–2.84 Ga, with the metamorphic age of 2.7 Ga [*Levchenkov et al.,* 1995]. The gneisses are intruded by granite porphyry and granodiorite plutons (dated at ∼2.5 Ga) and granite and pegmatite dikes (2.7–2.5 Ga). The metamorphic grades of the rocks do not exceed the middle part of the amphibolite facies. According to deep seismic sounding results, rocks in the northwestern surroundings of the Pechenga structure can be traced beneath this structure and account for a significant part in its basement [*A seismological...,* 1997]. Analogous rock associations make up the eastern part of the Inari block [*Kesola,* 1991]. The Inari block and the Svanvik–Neiden segment of the Kola–Norwegian block seem to have composed a single granite–greenstone terrane in Late Archean time and were separated in the Early Proterozoic during the development of the Palmak–Pasvik–Pechenga–Imandra–Varzuga structure.

The Titovsky segment of the Central Kola block near Pechenga Bay of the Barents Sea is dominated by aluminous gneisses of the Kola Group, which trend to the northwest and extend to Norway, where they are referred to as the Jarfiord Gneiss. It is believed that the aluminous gneisses rested on a basement of banded enderbites and two-pyroxene crystalline schists (Hompen Gneiss), dated at 2902±9 Ma [*Levchenkov et al.,* 1995]. The aluminous gneisses, whose protoliths consisted of hydromica clays, sands, and clayey graywackes, were determined to have lateral metamorphic zoning with the metamorphic grade decreasing from northwest to southeast from the granulite to amphibolite facies [*Facies...,* 1977; *Vinogradov and Vinogradova,* 1993]. The age of the early metamorphism of the aluminous gneisses was constrained by a variety of techniques to the interval of 2.88–2.83 Ga [*Avakyan,* 1992; *Balashov et al.,* 1992], with the latest metamorphic episode dated at 2.7 Ga. The gneisses were determined to bear evidence of seven to eight folding events in the regime of subhorizontal or tangential motions [*Dobrzhinetskaya,* 1978]. The aluminous gneisses are intruded by rocks of the gabbro–tonalite (2.83 Ga), granodiorite (2.76–2.73 Ga), and monzonite–syenite (2.73 Ga) composition, which compose, respectively, pre-, syn-, and postmetamorphic intrusions [*Nordgulen et al.,* 1995; *Vetrin et al.,* 1995].

It follows that the composition and age of supracrustal rocks, their metamorphic grades, and the ages of intrusions are remarkably different in the Titovsky and Svanvik–Neiden segments. According to *Condie* [1981], they can be attributed to, respectively, the terranes of high-grade metamorphic (granulite gneissic) and granite–greenstone rocks. The former were produced at a contraction coupled with granulite metamorphism and emplacement of charnockite–enderbite intrusions, and the latter developed under crustal extension, in relation to the ascent of mantle material and reomorphism of the host rocks during the development of granite–greenstone terranes.

## Geologic Criteria for Correlations Between Rocks of the KSDB Archean Complex and Rocks in the Framing of the Pechenga Structure

### Rock Complexes

In the sequence penetrated by the Kola Superdeep Borehole, the Paleoproterozoic sedimentary–volcanic rocks of the Pechenga structure are underlain (at depths of 6842–12,261 m) by Archean rocks, which can be subdivided into five cyclic units. Each of them is, in turn, composed of two members, which are dominated by migmatized biotite–plagioclase gneisses of tonalite–trondhjemite composition (∼45%) and gneisses with high-Al minerals (gneisses with HAM, ∼20%), which originally correspond to volcanic and sedimentary rocks, respectively [*Archean...,* 1991; *Kola Superdeep Borehole,* 1984; *Kremenetsky and Ovchinnikov,* 1986]. About 30% of the sequence falls to amphibolites and iron quartzites (BIF), and ∼5% is accounted for by granitoid veins. In the lower part of the KSDB section, below a depth

of 11,708 m, an amphibolite–tonalite–trondhjemite complex (ATTC, Figure 2) was recognized. The Archean complex of KSDB was metamorphosed under amphibolite-facies (pre-Pechenga) conditions and, later, under low-temperature amphibolite, epidote amphibolite, and, more rarely, greenschist facies (Pechenga) conditions [*Duk et al.,* 1989; *Kola Superdeep Borehole,* 1984]. Some researchers believe that the Archean rocks of KSDB contain the most ancient granulite-facies relics [*Magmatic...,* 1986], but this hypothesis was not confirmed by later mineralogical [*Yakovleva,* 1991] and isotopic geochemical [*Chen et al.,* 1998] studies.

Metamorphism to the amphibolite- and epidote amphibolite facies of the late (Pechenga) episode was associated with migmatization of rocks of the Archean complex expressed in development of patchy, conformable, and, mostly, nebular migmatites. Their amounts are as high as 15–20% in the gneisses with aluminous minerals and increase upsection from 20–30% in the biotite–plagioclase gneisses of unit 10 to 50–60% in the gneisses of unit 2.

The age of the protoliths of the gneisses was constrained by isotopic geochemical techniques to 2950–2850 Ma, and the ATTC granitoids were dated at 2835–2832 Ma. Equal dates were determined for the tonalitic gneisses of units 1, 2, and 8. The gneisses with HAM are some 30–150 m.y. younger than the underlying tonalites–trondhjemites. The migmatites developed at approximately 2740 Ma, during the closing stages of the Late Archean metamorphic event. The Proterozoic migmatites were dated at 2225–2150 Ma, and the postkinematic veins of porphyritic and equally grained granites were intruded at 1766 Ma [*Bibikova et al.,* 1993; *Chen et al.,* 1998; *Timmerman and Daly,* 1995; *Yakovlev et al.,* 2000].

The data cited above come in conflict with the recognition of Early Archean rocks in the lower part of the succession penetrated by KSDB [*Vinogradova et al.,* 2000]; neither was confirmed the correlation between the upper part of the succession and the rocks of the greenstone tectonostratigraphic complex of the Vyrnimskaya and Tal'inskaya formations in the southern framing of the Pechenga structure [*Vinogradova et al.,* 2000], because the $T^{143}Nd/^{144}Nd(DM)$ model ages of the latter formations are no older than 2.3–2.4 Ga [*Pozhilenko et al.,* 2000].

It is expedient to search for associations analogous to the rocks of the KSDB Archean complex bearing in mind that the probable analogues should be coeval, have similar mineralogical and chemical compositions, be characterized by quantitatively similar rock proportions in the rock complexes, and have protoliths of similar composition. Obviously, none of the aforementioned features taken alone (for example, similarities in chemistry) cannot be put forth as a proof of an analogy between the rocks compared. It is equally inaccurate to compare rock complexes metamorphosed to distinct metamorphic facies, because a comparison of such complexes, whose rocks differ mineralogically, would require evidence of the preservation of their original chemistry under different $P-T$ conditions. In particular, this pertains to migmatized and granitized rock complexes metamorphosed to the amphibolite and granulite facies.

Another aspect that makes it difficult to compare the rocks exposed at the surface and those in the KSDB Archean complex is the transformation of the latter under the effect of the Early Proterozoic mantle–crust interaction, related to the development of the Pechenga riftogenic structure. Because of this, correlation between the KSDB Archean complex and complexes exposed at the surface remain ambiguous. The KSDB Archean complex is commonly paralleled with the gneisses of the Kola Group, which consists of two units: lower, composed of biotite–plagioclase gneisses with subordinate amounts of aluminous gneisses, amphibolites, magnetite–garnet–pyroxene schists, and iron quartzites; and upper, dominated by garnet–biotite–plagioclase gneisses with sillimanite, staurolite, and andalusite [*Kola Superdeep Borehole,* 1984; *Magmatic...,* 1986]. The aluminous gneisses of the upper unit are restricted mostly to the Titovsky segment of the Central Kola block, which consists of magmatic and metamorphic rocks of specific textures and compositions that have never been reliably identified in the KSDB rocks. Because of this, it seems to be useless to search for analogues of the KSDB Archean complex among the high-grade gneisses on the Barents seashore [*Guberman et al.,* 1994; *Kozlov et al.,* 2001], where there are virtually no tonalite–trondhjemite gneisses analogous to those dominating in the Archean complex of the borehole.

According to geological–geophysical data, certain similarities with the KSDB Archean complex are displayed by tonalite–trondhjemite gneisses with layers of aluminous gneisses and amphibolites that compose the Svanvik–Neiden segment of the Central Kola block. These rocks occur mostly in the northwestern, northeastern, and eastern framing of the Pechenga structure. In earlier schemes, the tonalite–trondhjemite gneisses and related amphibolites were considered to be the lower gneiss unit of the Kola Group [*Kola Superdeep Borehole,* 1984; *Magmatic...,* 1986] or the basement complex [*Radchenko et al.,* 1994]. We examined these rocks in much detail in the northwestern surroundings of the Pechenga structure, mainly in northern Norway.

In accordance with their geologic setting, textural and structural features, quantitative rock proportions, and deformation styles, the gneisses of the Svanvik–Neiden segment are subdivided into a series of complexes (Varanger, Svanvik, Garsjø, and others; [*Dobrzhinetskaya et al.,* 1995; *Siedleska et al.,* 1985]). The most diverse rock associations are typical of the Garsjø gneisses in the northwestern part of the area (Figure 1). This complex is dominated by biotite and more rare amphibole–biotite gneisses of tonalite-trondhjemitic composition (50–60%) with strata of garnet–biotite and sillimanite–garnet–biotite gneisses (10–20%) and amphibolites (10–20%) and iron quartzites layers. The amounts of migmatites and granite or pegmatite veins are, respectively, 10–20 and 5–10%. The U–Pb metamorphic age of the Garsjø gneisses was estimated at ∼2.7 Ga, and two fractions of magmatic zircon were dated at 2840 Ma [*Levchenkov et al.,* 1995]. The age and the rock assemblage of the Garsjø gneisses are most close to those of rocks in the KSDB Archean complex, differing from the latter by less intense migmatization and smaller volumes of mafic rocks [*Vetrin et al.,* 1999].

The Svanvik gneisses are exposed at the western contact with the Pechenga structure and compose an intrusive complex consisting of at least two phases. The predominant

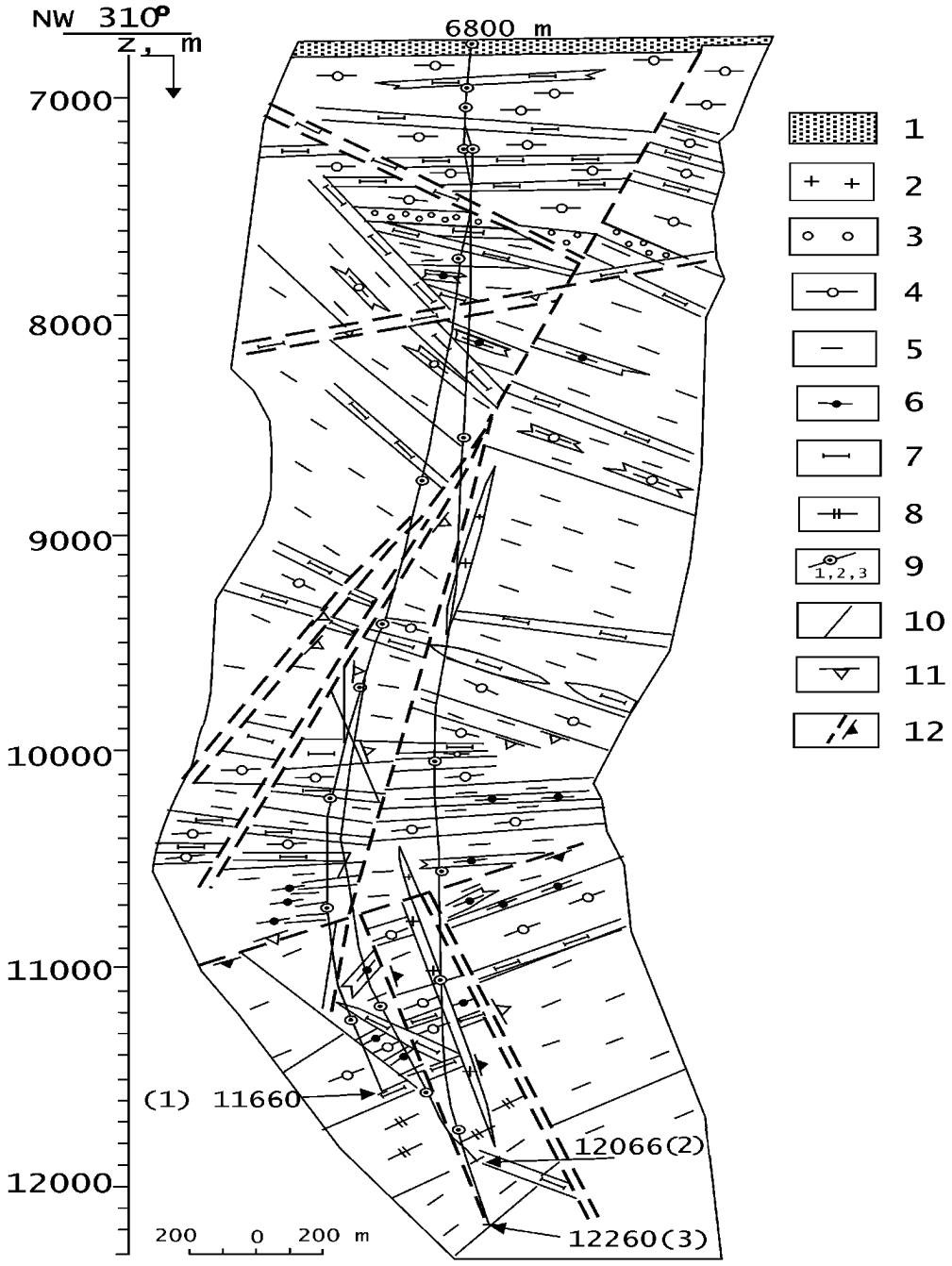


**Figure 2.** Archean complex in the basement of the Pechenga structure penetrated by the Kola Superdeep Borehole (simplified after [*Kola Superdeep Borehole,* 1998] and appended with authors' materials).
(1) Obliquely stratified sandstones with conglomerate layers; (2) postkinematic granites and pegmatites (Proterozoic); (3) metamorphosed weathering crust and conglomerates; (4) biotite–plagioclase gneisses with high-Al minerals; (5) biotite–(amphibole)–plagioclase gneisses; (6) Fe-quartzites, amphibole–magnetite–quartz schists; (7) para- and orthoamphibolites; (8) rocks of the amphibolite–tonalite–trondhjemite complex (ATTC); (9) numbers of borehole strings in chronological succession and their depths; (10) contacts of layers or bodies; (11) mylonitization, cataclasis, and brecciation; (12) faults and sutures.

rock types are banded tonalitic gneisses with layers and lens-shaped bodies of feldspar amphibolites. The rocks of the second phase are equally grained massive or unclearly gneissose tonalites. The U–Pb age of their magmatic crystallization is 2825±34 Ma [*Levchenkov et al.,* 1995].

The Varanger gneisses are separated from the Garsjo gneisses by a tectonized zone of northeastern trend. The dominant rocks of this complex are tonalite–trondhjemite gneisses with massive or fine- to coarse-banded structures. Their U–Pb isochron age was determined to be 2803–2813 Ma [*Levchenkov et al.,* 1995]. The tonalites contain enclaves of feldspathic and garnet-bearing amphibolites with iron quartzites (jaspilite) lenses, bodies of garnet–biotite, two-mica, and garnet–biotite–sillimanite gneisses. In places, the aluminous gneisses and associated amphibolite and iron quartzites (jaspilite) bodies compose greenstone structures (Valen, Bjørnvatn, and others) with conformable tectonized contacts with respect to the host tonalite–trondhjemite gneisses.

### Correlations

*Balashov and Vetrin* [1991] suggested that the KSDB Archean complex is an intensely migmatized and granitized fragment of an Archean granite–greenstone terrane. Its principal rock types are gneisses of tonalite-trondhjemitic composition in association with amphibolites, gneisses with HAM, and iron quartzites (jaspilites). The latter three rock types are, along with tonalite–trondhjemite, the predominant rock associations of Precambrian greenstone belts [*Condie,* 1981]. In the lower part of the sequence, the rocks recognized as the amphibolite–tonalite–trondhjemite complex (ATTC) have blastogranitic textures, are devoid of layering, and bear no layers of metasediments, that indicate plutonic precursors of tonalite–trondhjemite gneisses.

Analogous rock assemblages compose the Svanvik–Neiden segment of the Kola–Norwegian block. The tonalite–trondhjemite gneisses that are dominant in the Svanvik complex comprise a number of phases and in places retain relict porphyroblastic textures. The Garsjø and Varanger complexes are characterized by a clearly pronounced rock banding, defined by intercalating of tonalite-trondhjemitic gneisses with various proportions of mafic minerals, amphibolites, gneisses with HAM, and iron quartzites (jaspilites). The aforementioned structural and textural features of these rocks and their composition testify to the predominantly sedimentary–volcanogenic genesis of the main rock associations of the complexes and their crystallization under disequilibrium near surface conditions. The Garsjø and Varanger tonalite–trondhjemite gneisses include numerous relict bodies of amphibolites, gneisses with HAM, and iron quartzites (jaspilites). Their rock associations including BIF and composition are close to those of rocks in the Bjornevatn greenstone structure, and they seem to be relics of greenstone structures (possibly, of different ages), which were intruded by tonalite–trondhjemites.

## Petrography and Geochemistry

Presented below are the results of petrographic and geochemical examinations of the tonalite–trondhjemite gneisses, gneisses with HAM, and amphibolites, which are the principal rock types from the KSDB Archean complex and the framing of the Pechenga structure.

### Samples and Analytical Techniques

Samples of the KSDB core and rocks from the northwestern framing of the Pechenga structure were analyzed for major and trace elements by ICP-MS, ICP, INAA, XRF, and mass spectrometry at the Centre for Petrographic and Geochemical Researches (CRPG-CNRS) in Nancy, France (32 samples); United Institute of Geology, Geophysics, and Mineralogy, Siberian Branch, Russian Academy of Sciences, Novosibirsk, Russia (19 samples); Geological Institute, Kola Science Center, Russian Academy of Sciences, Apatity, Russia, and the Institute of the Mineralogy, Geochemistry, and Crystal Chemistry of Rare Elements, Moscow (accordingly, 4 and 7 samples). The Sm–Nd isotopic analyses of the rocks were conducted at the Laboratory of Geochronology at the Geological Institute, Kola Science Center. The results are summarized in Tables 1–8.

### Petrography

**Kola Superdeep Borehole.** The KSDB Archean complex is dominated by tonalite–trondhjemite gneisses, which are usually variably migmatized. To reproduce the primary characteristics of the rocks, we examined the least altered of their samples, mainly from the lower part of the sequence penetrated by the borehole (units 8 and 10). The plagiogneisses in question were subdivided into two types. One of them comprises mesocratic and more rare leucocratic varieties with granoblastic and blastogranitic textures. The mesocratic gneisses (Table 1, Samples 46a, 44895, 45001-3, 36305, 40302-2) consist of plagioclase (50–55%, 31–40% An), quartz (25–30%), and biotite (10–15%); Sample 45001-3 contains both biotite and hornblende. The leucocratic gneisses (Samples 39866-6, 39288-6 and Sample 36009 of microclinized gneiss) contain 5–10% biotite and 60–65% plagioclase (24–27% An). The accessory minerals of all rocks are magnetite, ilmenite, apatite, zircon, sphene, and allanite. The gneisses of the second type (Samples 30085/1a and 34944) are higher in biotite (up to 20%) or muscovite and epidote, which replace primary mineral assemblages.

The gneisses with HAM are characterized by the absence of potassic feldspar and the strong dominance of micas over aluminous minerals. Our samples represented two-mica gneisses with sillimanite (Table 2, Samples 22627 and 37926) and garnet–biotite gneisses (Sample 41426-3).

In accordance with their geologic setting and composition, the orthoamphibolites were subdivided into rocks of the dike facies (predominant type; Table 3), metapyroxenite (Sample

**Table 1.** Concentrations of major and trace elements (wt % and ppm, respectively) in Kola Super Deep Hole plagiogneisses

| Geoch. type | A | | | | | | | | B | |
|---|---|---|---|---|---|---|---|---|---|---|
| Sample, no. | 46a** | 44895** | 45001-3 | 36305 | 39866-6** | 36009 | 40302-2** | 39288-6 | 30085/1A* | 34944** |
| Depth, m | 11852 | 12148 | 12218 | 9802 | 10865 | 9570 | 11045 | 10593 | 8568 | 9313 |
| $SiO_2$ | 67.66 | 68.81 | 69.97 | 69.65 | 71.47 | 72.07 | 66.29 | 71.94 | 65.31 | 70.38 |
| $TiO_2$ | 0.35 | 0.5 | 0.39 | 0.28 | 0.43 | 0.15 | 0.42 | 0.19 | 0.81 | 0.57 |
| $Al_2O_3$ | 15.54 | 15.66 | 15.23 | 16.18 | 14.72 | 15.43 | 18.65 | 15.65 | 16.98 | 15.15 |
| $Fe_2O_3$ | 4.71 | 3.70 | 3.26 | 2.74 | 2.60 | 1.18 | 2.50 | 2.0 | 4.75 | 2.40 |
| MnO | 0.05 | 0.05 | – | – | 0.04 | – | 0.04 | – | 0.04 | 0.01 |
| MgO | 1.15 | 1.15 | 1.01 | 0.87 | 0.75 | 0.35 | 1.17 | 0.5 | 1.43 | 0.97 |
| CaO | 3.74 | 3.86 | 3.95 | 2.83 | 2.93 | 1.63 | 4.11 | 3.06 | 2.06 | 2.11 |
| $Na_2O$ | 4.66 | 3.45 | 4.01 | 5.45 | 4.31 | 5.04 | 4.98 | 5.11 | 5.5 | 5.1 |
| $K_2O$ | 1.16 | 1.35 | 1.24 | 1.23 | 1.19 | 3.33 | 1.35 | 1.0 | 1.55 | 1.75 |
| $P_2O_5$ | 0.13 | – | 0.13 | 0.09 | 0.08 | 0.08 | 0.04 | 0.09 | 0.24 | 0.13 |
| LOI | 0.77 | 0.95 | 0.62 | 0.5 | 0.89 | 0.65 | 0.47 | 0.25 | 1.05 | 1.38 |
| Total | 99.92 | 99.48 | 99.81 | 99.82 | 99.41 | 99.91 | 100.02 | 99.79 | 99.72 | 99.95 |
| U | | | 0.50 | 0.43 | | 6.8 | | | | |
| Th | | | 3.4 | 0.9 | | 6.0 | | 0.12 | 21 | 12 |
| Rb | 71 | 113 | 61 | 81 | 51 | 91 | 110 | 51 | 50 | 80 |
| Ba | 415 | | 382 | 326 | | 1179 | | 133 | 140 | 310 |
| Sr | 262 | 247 | 249 | 441 | 433 | 449 | 541 | 300 | 90 | 300 |
| La | 24.77 | 13.33 | 22.8 | 10.1 | 35.99 | 15.9 | 4.56 | 5.5 | 65 | 44 |
| Ce | 42.37 | 36.09 | 40.0 | 18.8 | 76.56 | 28.4 | 9.65 | 9.1 | 140 | 68 |
| Pr | | | 4.0 | 2.0 | | 2.8 | | 0.9 | | |
| Nd | 12.8 | 11.91 | 12.3 | 7.4 | 25.71 | 9.4 | 4.98 | 3.3 | | |
| Sm | 1.77 | 2.12 | 1.7 | 1.4 | 4.71 | 1.4 | 1.28 | 0.6 | 5.8 | 2.9 |
| Eu | 0.616 | 1.87 | 0.70 | 0.44 | 2.00 | 0.60 | 0.50 | 0.51 | 1.4 | 0.93 |
| Gd | 1.24 | 1.79 | 1.0 | 1.1 | 1.98 | 1.0 | 1.28 | 0.5 | | |
| Tb | | | 0.13 | 0.19 | | 0.12 | | 0.06 | 0.78 | 0.3 |
| Dy | 0.77 | 1.326 | 0.65 | 0.94 | 0.920 | 0.47 | 1.056 | 0.26 | | |
| Ho | | | 0.11 | 0.18 | | 0.06 | | 0.04 | | |
| Er | 0.364 | 0.617 | 0.28 | 0.46 | 0.353 | 0.15 | 0.546 | 0.12 | | |
| Tm | | | 0.04 | 0.06 | | 0.02 | | 0.01 | | |
| Yb | 0.319 | 0.486 | 0.29 | 0.34 | 0.292 | 0.12 | 0.479 | 0.10 | 1.2 | 0.86 |
| Lu | | 0.072 | 0.05 | 0.05 | 0.042 | 0.02 | 0.068 | 0.02 | 0.18 | 0.13 |
| Zr | 132 | 168 | 185 | 116 | 178 | 94 | 86 | 94 | 200 | 100 |
| Hf | | | 4.0 | 2.8 | | 2.4 | | 2.7 | | |
| Ta | | | 0.26 | 0.23 | | 0.21 | | 0.14 | | |
| Nd | 13 | <7 | 4.4 | 2.9 | <7 | 1.5 | 7.0 | 3.9 | 10 | 3 |
| Y | 7 | <6 | 3.2 | 5.1 | <6 | 1.8 | <6 | 1.3 | | |
| Cr | 10 | 4 | 9 | 16 | 4 | 13 | 3 | 6 | 25 | 22 |
| Ni | 20 | 12 | 11 | 11 | 6 | – | 8 | – | 7 | 5 |
| Co | 5 | <10 | 8 | 7 | 8 | 2 | 10 | 3 | 5 | 2.2 |
| V | 40 | 54 | 36 | 33 | 35 | 13 | 61 | 17 | 48 | – |
| $(La/Yb)_n$ | 52.16 | 18.5 | 52.4 | 20.2 | 83.1 | 90.4 | 6.4 | 36.1 | 36.5 | 34.5 |
| $Eu/Eu^*$ | 1.21 | 2.86 | 1.51 | 1.07 | 1.71 | 1.47 | 1.19 | 2.95 | | |

Note: Here and in tables below, * mark analyses conducted at the UIGGM RAS, Novosibirsk; ** mark analyses conducted at GI KSC RAS, Apatity and IMGRE, Moscow; other analyses were carried out at CRPG-CNRS, Nancy, France: empty cells – not analyzed, dashes – not determined.

9608), garnet–clinopyroxene metagabbro (Sample 43745), and cummingtonite–hornblende metagabbro (Table 5, Sample 27023). The dike rocks are feldspathic amphibolites and, more rarely, garnet–feldspar amphibolites (Sample 42167). The most common textures of the rocks are nematoblastic and granonematoblastic; samples 42167 and 44369-2 show relict ophitic, poikilitic, and allotriomorphic-granular textures.

**Table 2.** Concentrations of major and trace elements (wt % and ppm, respectively) in gneisses with HAM from KSDB and the Garsjø Complex

| Complex | KSDB | | | Garsjø | | | | | |
|---|---|---|---|---|---|---|---|---|---|
| Sample, no. | 22627 | 37926 | 41426-3 | 70-3 | 68-5 | 46/99* | 68-1 | 16/99* | 80-1 |
| Depth, m | 6905 | 10210 | 11418 | | | | | | |
| $SiO_2$ | 50.99 | 62.41 | 74.69 | 52.31 | 54.67 | 59.02 | 61.54 | 66.53 | 70.51 |
| $TiO_2$ | 0.89 | 0.67 | 0.4 | 1.44 | 0.77 | 0.659 | 0.71 | 0.431 | 0.56 |
| $Al_2O_3$ | 22.23 | 17.57 | 12.13 | 14.97 | 17.68 | 15.69 | 14.67 | 15.17 | 14.33 |
| $Fe_2O_3$ | 7 | 6.59 | 3.67 | 13.09 | 8.47 | 8.56 | 6.89 | 6.18 | 4.86 |
| MnO | 0.9 | 0.06 | – | 0.15 | 0.12 | 0.122 | 0.11 | 0.088 | 0.04 |
| MgO | 5.23 | 2.47 | 1.66 | 4.5 | 4.98 | 3.33 | 3.12 | 1.88 | 2.17 |
| CaO | 4.67 | 2.27 | 2.63 | 6.97 | 7.47 | 5.5 | 4.83 | 1.63 | 1.63 |
| $Na_2O$ | 4.37 | 4.4 | 2.74 | 3.21 | 1.96 | 3.43 | 2.35 | 3.75 | 2.84 |
| $K_2O$ | 3.38 | 2.75 | 1.46 | 2.17 | 2.01 | 2.62 | 3.17 | 1.57 | 2.13 |
| $P_2O_5$ | 0.11 | 0.09 | 0.05 | 0.23 | 0.2 | 0.128 | 0.19 | 0.058 | 0.08 |
| LOI | 1.04 | 0.61 | 0.34 | 0.85 | 1.49 | 0.96 | 2.25 | 2.13 | 0.71 |
| Total | 100 | 99.89 | 99.77 | 99.89 | 99.82 | 100 | 99.83 | 99.42 | 99.86 |
| U | 3.6 | 1.4 | 0.6 | 0.63 | 0.67 | 1.5 | 1.90 | 7.5 | 2.12 |
| Th | 13.5 | 7.5 | 2.4 | 6.2 | 2.6 | 5.4 | 8.5 | 6.3 | 6.2 |
| Rb | 171 | 119 | 44 | 76 | 134 | 150 | 181 | 184 | 98 |
| Ba | 1056 | 510 | 119 | 480 | 162 | 530 | 239 | 265 | 450 |
| Sr | 749 | 334 | 33 | 357 | 157 | 248 | 149 | 275 | 212 |
| La | 46.1 | 23.9 | 12.1 | 39.6 | 17.1 | 21 | 28.7 | 25 | 25.7 |
| Ce | 89.3 | 48.4 | 23.7 | 85.4 | 34.7 | 40 | 59.3 | 42 | 50.9 |
| Pr | 10.3 | 5.4 | 2.4 | 10.4 | 4.4 | | 7.0 | | 5.8 |
| Nd | 38.4 | 19.8 | 8.2 | 40.2 | 17.4 | 18 | 26.3 | 21 | 20.5 |
| Sm | 6.3 | 3.0 | 1.5 | 7.2 | 4.1 | 3.5 | 5.1 | 3.4 | 3.8 |
| Eu | 1.59 | 1.10 | 0.44 | 1.91 | 1.27 | 0.95 | 1.16 | 0.72 | 1.02 |
| Gd | 5.1 | 2.0 | 1.1 | 5.9 | 4.5 | 2.4 | 4.2 | 1.9 | 3.0 |
| Tb | 0.65 | 0.27 | 0.17 | 0.82 | 0.67 | 0.47 | 0.63 | 0.43 | 0.40 |
| Dy | 3.49 | 1.30 | 0.85 | 4.4 | 4.0 | | 3.8 | | 2.4 |
| Ho | 0.55 | 0.20 | 0.16 | 0.79 | 0.86 | | 0.75 | | 0.46 |
| Er | 1.43 | 0.55 | 0.45 | 1.9 | 2.5 | | 2.0 | | 1.4 |
| Tm | 0.18 | 0.08 | 0.06 | 0.27 | 0.40 | | 0.32 | | 0.23 |
| Yb | 1.11 | 0.48 | 0.43 | 1.7 | 2.5 | 1.7 | 2.1 | 1.04 | 1.5 |
| Lu | 0.17 | 0.08 | 0.07 | 0.23 | 0.40 | 0.27 | 0.32 | 0.16 | 0.22 |
| Zr | 173 | 133 | 103 | 186 | 135 | 143 | 156 | 121 | 180 |
| Hf | 4.7 | 3.4 | 2.5 | 4.4 | 3.4 | 3.2 | 3.9 | 3.1 | 4.8 |
| Ta | 0.61 | 0.65 | 0.32 | 0.77 | 0.56 | 0.5 | 0.65 | 1 | 0.48 |
| Nb | 6.5 | 8.4 | 3.2 | 12.2 | 5.9 | 3.8 | 6.2 | 15.1 | 5.1 |
| Y | 15.0 | 6.1 | 4.4 | 21.4 | 25.1 | 17.7 | 20.7 | 16 | 12.9 |
| Cr | 354 | 170 | 135 | 86.0 | 134.2 | 40 | 89.5 | 110 | 186.7 |
| Ni | 184 | 81 | 51 | 76.8 | 72.9 | | 66.1 | | 32.1 |
| Co | 35 | 24 | 14 | 37.3 | 24.4 | 20 | 20.3 | 21.5 | 13.4 |
| V | 136 | 130 | 75 | 134 | 152 | | 125 | | 96 |
| $(La/Yb)_n$ | 28.1 | 33.5 | 18.8 | 16.0 | 4.7 | 8.3 | 9.4 | 16.2 | 11.4 |
| $Eu/Eu^*$ | 0.84 | 1.31 | 1.00 | 0.87 | 0.90 | 0.95 | 0.74 | 0.79 | 0.90 |

**Complexes Exposed at the Surface.** The plagiogneisses generally have granoblastic or, more rarely, porphyroblastic and blastogranitic textures. In contrast to the analogous rocks from KSDB, these plagiogneisses are characterized by relict porphyritic textures with plagioclase and quartz phenocrysts. The Svanvik gneisses, which occur in contact with the Pechenga structure, are locally microclinized, muscovitized, and chloritized. The main minerals of the plagiogneisses are plagioclase (23–40% An), quartz, and biotite, with hornblende encountered only in the most melanocratic varieties (Table 6, Samples 56-1, 65-15, 91-170, and 90-30). The accessories are epidote, allanite, apatite, zircon, magnetite, ilmenite, and, occasionally, sphene.

The gneisses with HAM have granoblastic, porphyrogra-

**Table 3.** Concentrations of major and trace elements (wt % and ppm, respectively) in amphibolites of types I (1–4) and II (5–6) from the KSDB Archean complex and in the Pechenga metabasalts recovered by KSDB (7–10)

| 1 | 2 | 3 | 4 | 5 | 6 | 7 | 8 | 9 | 10 |
|---|---|---|---|---|---|---|---|---|---|
| 31375 | 36582 | 44369-2 | 42167 | 24744/2** | 33687/1** | 3173 | 13082 | 18761 | 21846 |
| 8803 | 9901 | 12020 | 11662 | 7645-51 | 9051-64 | 1047.4 | 3422,7 | 5116.5 | 6663 |
| 49.15 | 49.28 | 48.34 | 51.17 | 48.82 | 49.1 | 46.88 | 43.57 | 49.85 | 53.97 |
| 2.11 | 1.86 | 1.94 | 1.91 | 0.85 | 0.76 | 1.23 | 1.98 | 1.89 | 0.8 |
| 13.46 | 13.42 | 13.58 | 13.91 | 14.49 | 13.52 | 14.29 | 15.46 | 16.6 | 14.04 |
| 17.55 | 16.49 | 17.48 | 17.99 | 13.58 | 13.86 | 13.69 | 17.45 | 16.35 | 10.2 |
| 0.25 | 0.24 | 0.23 | 0.32 | 0.18 | 0.23 | 0.2 | 0.21 | 0.22 | 0.15 |
| 4.36 | 5.18 | 4.76 | 5.24 | 7.9 | 6.75 | 7.56 | 6.56 | 2.62 | 6.32 |
| 9.38 | 10.39 | 9.86 | 8.99 | 9.76 | 11.61 | 10.63 | 9.03 | 3.31 | 7.62 |
| 1.94 | 1.92 | 2.43 | 0.65 | 2.1 | 2 | 2.05 | 1.73 | 6.55 | 3.3 |
| 1.71 | 1.05 | 0.8 | 0.2 | 1.25 | 0.6 | 0.54 | 0.13 | 1.41 | 1.43 |
| 0.24 | 0.23 | 0.23 | 0.22 | 0.09 | 0.07 | 0.15 | 0.21 | 0.16 | 0.15 |
| 0.28 | 0.39 | 0.21 | −0.36 | 1.38 | 1.67 | 2.66 | 3.54 | 0.87 | 1.89 |
| 100.43 | 100.45 | 99.86 | 100.24 | 100.4 | 100.17 | 99.88 | 99.87 | 99.83 | 99.87 |
| 0.85 | 0.79 | 0.58 | 0.94 | <2 | <2 | 0.18 | 0.44 | 83 | 7.46 |
| 3.5 | 3.1 | 3.6 | 3.3 | | <1.6 | 0.39 | 1.74 | 2.51 | 28.1 |
| 48.2 | 42.6 | 11.3 | 2.6 | 40.0 | | 12.4 | 2.82 | 44 | 621 |
| 306 | 148 | 182 | 24 | | 40 | 156 | 78.8 | 230 | 3892 |
| 174 | 198 | 253 | 58 | 100 | 100 | 393 | 326 | 118 | 2264 |
| 24.4 | 22.6 | 28.0 | 21.7 | 3.6 | 3.7 | 3.75 | 14.8 | 13.5 | 154 |
| 53.8 | 52.6 | 60.8 | 50.7 | 7.75 | 7.8 | 9.97 | 35.6 | 32.4 | 322 |
| 6.8 | 6.6 | 7.3 | 6.6 | | | 1.49 | 4.72 | 4.47 | 39.4 |
| 27.1 | 27.7 | 29.1 | 27.7 | | | 7.99 | 21.2 | 19.6 | 157 |
| 5.9 | 5.8 | 5.8 | 6.0 | 1.9 | 1.7 | 2.63 | 5.09 | 4.49 | 31.8 |
| 1.72 | 1.76 | 1.37 | 1.84 | 0.9 | 0.76 | 1.06 | 1.73 | 1.47 | 9.63 |
| 6.0 | 5.9 | 5.8 | 6.0 | | | 3.56 | 5.51 | 4.62 | 32.4 |
| 0.91 | 0.88 | 0.89 | 0.91 | 0.63 | 0.45 | 0.556 | 0.852 | 0.713 | 4.99 |
| 5.71 | 5.26 | 5.17 | 5.61 | | | 3.58 | 5.69 | 4.44 | 30.6 |
| 1.13 | 1.01 | 1.00 | 1.13 | | | 0.759 | 1.15 | 0.85 | 5.86 |
| 2.97 | 2.88 | 2.59 | 3.08 | | | 2.23 | 3.15 | 2.39 | 15.4 |
| 0.45 | 0.41 | 0.41 | 0.44 | | | 0.32 | 0.505 | 0.383 | 2.53 |
| 2.92 | 2.67 | 2.75 | 3.16 | 2.2 | 2.5 | 2.14 | 3.39 | 2.46 | 16 |
| 0.48 | 0.39 | 0.42 | 0.49 | 0.41 | 0.39 | 0.312 | 0.55 | 0.364 | 2.52 |
| 153 | 164 | 173 | 169 | 40 | 20 | 69 | 132 | 143 | 951 |
| 3.9 | 3.7 | 4.2 | 3.9 | | 1.5 | 1.84 | 3.52 | 3.77 | 25.2 |
| 1.45 | 1.21 | 1.37 | 1.40 | | | 0.27 | 0.93 | 0.89 | 3.39 |
| 18.7 | 16.6 | 18.3 | 19.8 | 1.5 | 3 | 3.46 | 12.2 | 11.6 | 42.1 |
| 30.8 | 29.3 | 30.1 | 32.7 | <20 | 40 | 22.1 | 34 | 25.5 | 167 |
| 45 | 69 | 16 | 60 | 120 | 60 | 260 | 181 | 164 | 2353 |
| 37 | 66 | 49 | 48 | 100 | 54 | 131 | 80.9 | 74.9 | 752 |
| 49 | 54 | 58 | 49 | 50 | 34 | 54.9 | 53.1 | 42.8 | 394 |
| 425 | 414 | 329 | 409 | | | 336 | 554 | 227 | 2111 |
| 4.90 | 4.96 | 3.79 | 2.31 | 10 | 13 | 1.2 | 2.75 | 3.58 | 25.1 |
| 5.6 | 5.7 | 6.9 | 4.6 | 1.1 | | 1.2 | 2.9 | 3.7 | 6.5 |

noblastic, and nematoblastic textures and typically exhibit broad variations in the contents of rock-forming minerals, which determines transitions from melanocratic amphibole–biotite gneisses with muscovite and sillimanite (Table 2, Samples 70-3, 68-5) to biotite and two-mica gneisses with sillimanite (Samples 46/99 and 68/1), garnet (Sample 16/99), and sillimanite plus garnet plus biotite (Sample 80-1).

The feldspathic amphibolites generally have a less variable composition than that of rocks from the KSDB Archean complex and consist of plagioclase (40–50%), amphibole, and, locally, biotite (≥10%). The accessory minerals are sphene, magnetite, apatite, and occasional allanite. The textures of the rocks are nematoblastic and granonematiblastic. The amphibolites hosted by the Svanvik gneisses

(Samples 109-2 and 107/99) are biotitized, epidotized, and carbonatized.

## Geochemistry

### Kola Superdeep Borehole

*Plagiogneisses.* The KSDB biotite plagiogneisses correspond to tonalite and, more rarely, trondhjemite in major element and normative composition (Table 1). Most of the rocks contain >15% $Al_2O_3$ at 70% $SiO_2$, have low $K_2O/Na_2O$ ratios, and high CaO concentrations, which are typical of Archean tonalite–trondhjemite–granodiorite series (TTG) [*Barker,* 1979]. According to their mineralogical, major-, and trace-element composition, the rocks can be classed into two types. The predominant gneisses of type A correspond to high-Al TTG. They are characterized by a strongly fractionated REE patterns, $(La/Yb)_n$ = 18–83, with a moderate enrichment in LREE, $La_n$ = 33–116, and a depletion in HREE, $Yb_n$ = 1.4–2.3, with unclear Eu anomalies (or without them, Figure 3a), which is typical of Archean TTG [*Martin,* 1994]. A microlcinized gneiss (Sample 36009) has REE and Zr, Hf, Ta, Nb, Y (i.e., HFSE – high field strength element) concentrations similar to those in the gneisses but differs from them by elevated contents of Ba. There are two noteworthy exceptions. Sample 39288-6 is low in LREE and shows a weakly fractionated REE pattern with a pronounced Eu maximum (Figure 3b). Its high $SiO_2$ concentration is associated with depletion in mafic components and HFSE, which was due to the low concentrations of mafic and accessory minerals. These compositional features seem to have been resulted from the fractional crystallization of the parental melt. The other exception, Sample 40302-2, represents more melanocratic rocks with a higher plagioclase content and low concentrations of accessory minerals. These compositional features can, perhaps, be interpreted as reflecting of the origin of the protolith as a plagioclase-enriched migmatite leucosome.

Gneisses of the other type (type B) were encountered in unit 2, which was thoroughly sampled by A. A. Kremenetsky, who provided us with the analyses of these gneisses cited in this paper. Gneisses of type A dominate in this unit [*Kremenetsky and Ovchinnikov,* 1986]. Compared with the gneisses of type A, which have the same $SiO_2$ concentrations, these rocks are enriched in Ti, Fe, Mg, REE ($La_n$ = 142–210, $Yb_n$ = 4.1–5.7), and HFSE (Figures 3c, 4c), which are concentrated in mafic and accessory minerals. The rocks are characterized by a weakly fractionated REE patterns, a feature generally uncommon for the gneisses of type A and typical Archean high-Al TTG. The multi-element patterns of these gneisses normalized to the primitive mantle have gentler slopes for the gneisses of type B. The rocks have pronounced Sr minima, which are also atypical of Archean grey gneisses (Figure 4c).

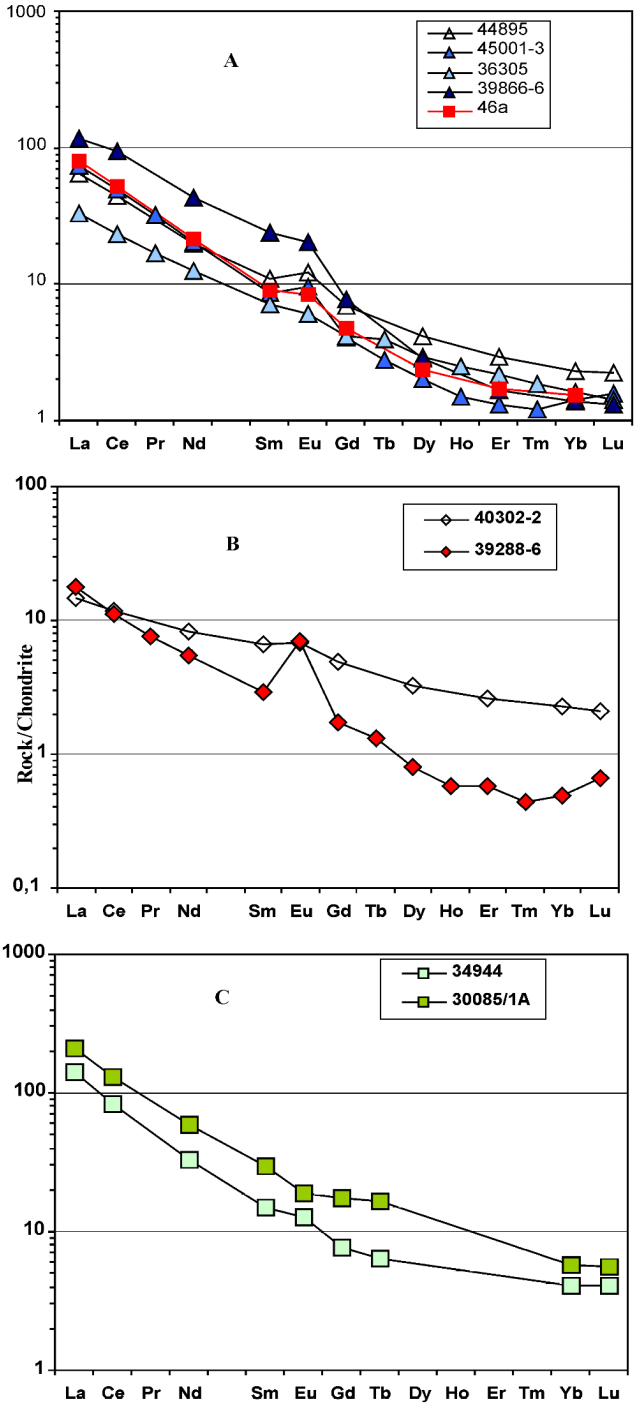


**Figure 3.** Chondrite-normalized [*Boynton,* 1984] REE patterns of tonalite–trondhjemite gneisses penetrated by KSDB.
A – geochemical type A; B – Samples 40302-2 and 39288-6 (see text); C – geochemical type B.

*Gneisses with High-Al Minerals.* The gneisses with HAM are characterized by broad variations in silica contents (Table 2, 51–75%), a component negatively correlated with most other elements. The rocks show fractionated REE patterns and a decrease in their concentrations with increasing $SiO_2$ contents. Another distinctive feature of the gneisses is their enrichment in LREE and HFSE, as well as relatively high concentrations of Cr, Ni, Co, and V. These data are gener-

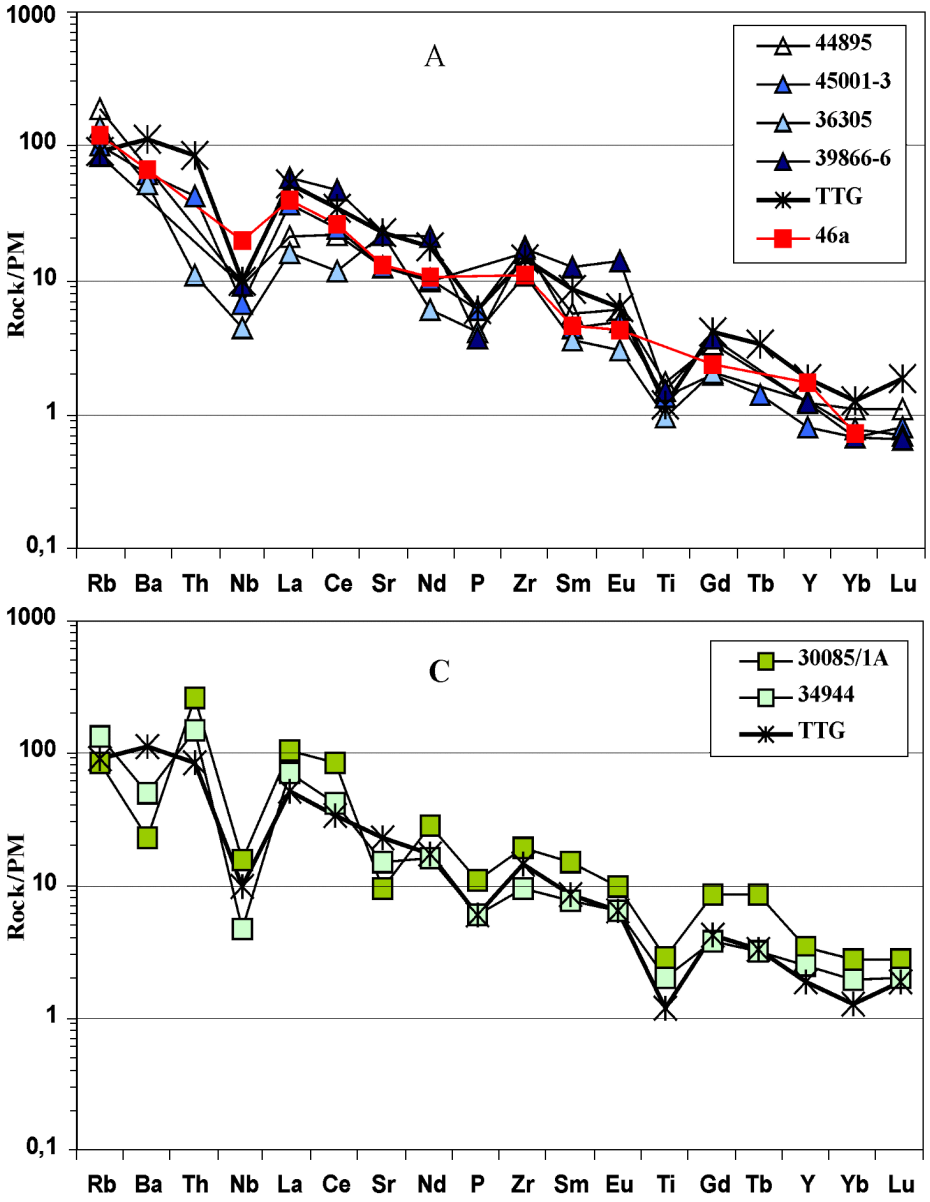


**Figure 4.** Trace-element concentrations normalized to the primitive mantle [*Sun and McDonough,* 1989] in the KSDB tonalite–trondhjemite gneisses. A – geochemical type A; C – geochemical type B.

ally consistent with the sedimentary nature of the protoliths of these rocks, which could consist of rocks of argillite–aleurolite composition. Compared to typical Archean shales [*Taylor and McLennan,* 1985], the gneisses with HAM are depleted in HREE and are characterized by higher $(La/Yb)_n$ = 19–33 ratios (Figure 5), which is most probably explained by the significant contribution of grey gneiss source to the origin of these sedimentary rocks.

*Amphibolites* In terms of normative composition, the amphibolites of the dike facies correspond to olivine tholeiite (four samples) or quartz tholeiite (two samples; Table 3). According to A. A. Kremenetsky, rocks of this type account for 70–80% of amphibolites in the KSDB Archean complex, belong to Fe-amphibolites, and form a part of the Late Archean volcano–plutonic tholeiite association. Some dike rocks of analogous composition were suggested to generated synchronously with the Pechenga volcanism [*Kremenetsky and Ovchinnikov,* 1986]. The occurrence of Proterozoic amphibolites among gneisses of the KSDB Archean complex is confirmed by zircon age (1836±161 Ma) of an amphibolite from a depth of 11,795 m [*Bibikova et al.,* 1993].

As follows from Table 3, the dike amphibolites are classed into two distinct types based on their compositional features. The amphibolites of the first type are characterized by a moderately fractionated REE patterns at elevated concentrations of LREE ($(La/Yb)_n$ = 4.6–6.9, $La_n$ = 70–90; Fig-

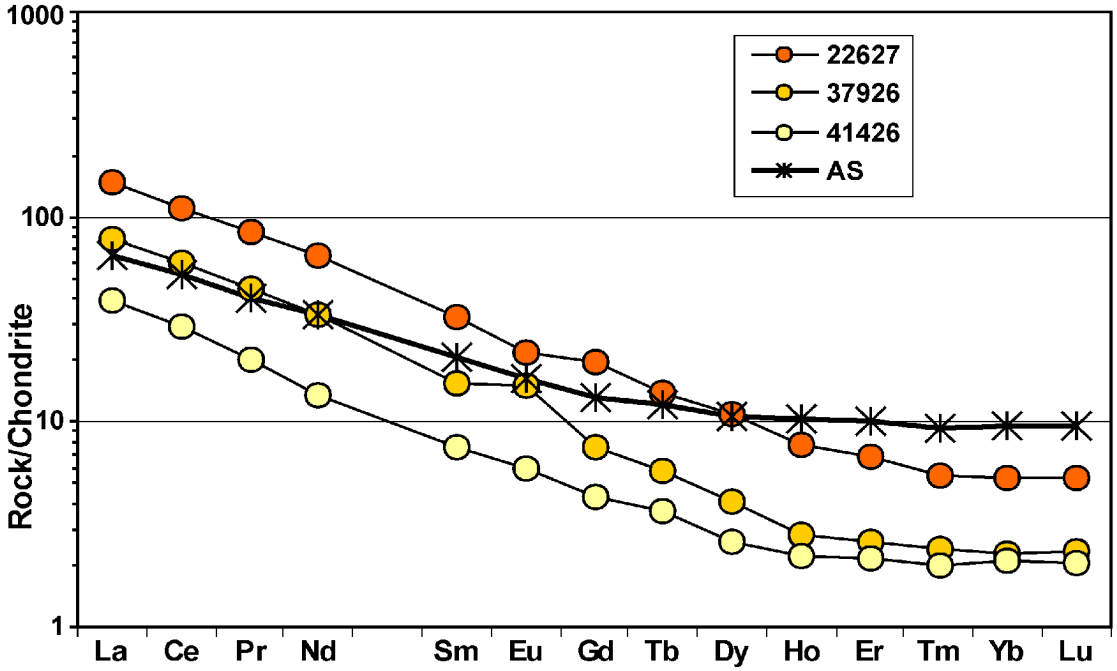


**Figure 5.** Chondrite-normalized REE patterns of gneisses with HAM penetrated by KSDB. AS – average Archean schist [*Taylor and McLennan,* 1985].

ure 6). The amphibolites of the second type are depleted in LREE ($La_n$ = 12–29), have flat REE patterns ($(La/Yb)_n$ = 1.0–1.1; Figure 7a), and are poorer in Fe, Ti, Th, Nb, and Zr and richer in Mg, Ni, and Pb than the first-type amphibolites.

Compared to Archean amphibolites from the surroundings of the borehole, the first-type amphibolites are enriched in REE and HFSE, exhibit more fractionated REE patterns (Figures 6, 8). They differ from REE-enriched TH2 basalts of Archean greenstone belts [*Condie,* 1981] by even higher concentrations of REE, $Fe_2O_3$, $TiO_2$, and V but lower concentrations of MgO and Cr, which could be explained by the derivation of basalt protoliths by the fractionation of a more primitive, Mg-rich melt. Among the Pechenga metavolcanics, rocks most closely approaching the amphibolites in terms of concentrations of REE and other trace elements, particularly HREE and HFSE, are the melanocratic basalts of the Zapolyarnyi Formation and the trachybasalts of the Pirttijarvi Formation (Figure 6, Table 3). At the same time, the latter have elevated concentrations of $Al_2O_3$ and $Na_2O$, relatively low contents of CaO and MgO at $SiO_2$ similar to those of the amphibolites, a feature incompatible with the concept that the amphibolites and Pirttijarvi basalts were produced by the differentiation of the same melt. A composition most similar to that of the KSDB amphibolites was identified in the basalts of the Zapolyarny Formation, which were derived from a relatively shallow source with an age of approximately 2.1 Ga [*Kola Superdeep Borehole,* 1998].

The revealed compositional similarities between the metavolcanic rocks of the Early Proterozoic Pechenga structure and amphibolites from the KSDB Archean complex are confirmed by the results obtained on the Sm–Nd systematics. The maximum model age of the amphibolites calculated under the assumption of the depleted composition of the regional mantle, $T_{Nd}(DM)$, is 2.16–2.33 Ga (Table 4), that determines the lower age limit for the origin of the protoliths. Given the compositional similarities between the amphibolites and the Zapolyarnyi metavolcanics in the Pechenga structure, which were dated at 2114±52 Ma [*Smolkin et al.,* 1995], we assumed the same age for the amphibolites analyzed. For this age, the $\varepsilon_{Nd}$ value of the amphibolites is 0.77–2.69, i.e., close or lower than the $\varepsilon_{Nd} \sim 3.5$ for the depleted mantle with an age of 2.1 Ga [*DePaolo,* 1981] (Figure 9). Lower $\varepsilon_{Nd}$ values are usually interpreted based on the assumption of either the enriched nature of the source or the contamination of the melts with upper crustal material [*Faure,* 1986]. The latter interpretation is in conflict with relatively low concentrations of Rb, Ba, and Pb in the Zapolyarnyi basalts. Hence, the $\varepsilon_{Nd}$ values calculated for the first-group amphibolites most probably reflect the derivation of the parental melts from a moderately depleted mantle source, insignificantly enriched in incompatible elements.

For the Pirttijarvi trachybasalts, which were dated at 2214±54 Ma [*Smolkin et al.,* 1995], the model age $T_{Nd}(DM)$ = 2460 Ma and $\varepsilon_{Nd}$ = 0.93, which lies within the range of $\varepsilon_{Nd}$ values determined for the amphibolites from the KSDB Archean complex.

In contrast to the first-type amphibolites, the second-type amphibolites have major- and trace-element compositions obviously similar to those of amphibolites from the surroundings of the borehole and the TH1 primitive tholeiites of Archean greenstone belts [*Condie,* 1981]. These similarities are further supported by the near flat REE patterns, relatively low concentrations of Ti, P, LREE ($La_n$ = 11.6–

**Table 4.** Sm–Nd systematics of rocks from KSDB and its surroundings

| Sample | Rock | Complex | Geoch. Type | [Sm], ppm | [Nd], ppm | $^{147}Sm/^{144}Nd$ | $^{143}Nd/^{144}Nd \pm 2s$ | T(DM),Ma | Tchur,Ma | Nd(0) | $\varepsilon$Nd(DM) | T, Ma* | Reference |
|---|---|---|---|---|---|---|---|---|---|---|---|---|---|
| 39288-6 | plagiogneiss | KSDB | A | 0.78 | 4.08 | 0.1153 | 0.511165±4 | 2915 | 2738 | 0.50895 | 0.9 | 2830 | Our data |
| 28 | ” | ” | | 1.94 | 12.63 | 0.0929 | 0.510736±16 | 2912 | 2774 | 0.50895 | 0.69 | ” | [*Timmerman and Daly,* 1995] |
| 46a | ” | ” | A | 2.02 | 14.52 | 0.0839 | 0.510562±14 | 2913 | 2786 | 0.50895 | 0.58 | ” | ” |
| 48 | ” | ” | | 2.40 | 13.74 | 0.1055 | 0.511043±12 | 2818 | 2648 | 0.50908 | 2.10 | ” | ” |
| 44369-2 | amphibolite | ” | | 4.7 | 22.56 | 0.12605 | 0.511695±4 | 2334 | 2023 | 0.50976 | 0.77 | 2114 | Our data |
| 42167 | ” | ” | | 5.6 | 26.9 | 0.12582 | 0.511790±9 | 2160 | 1814 | 0.51000 | 2.69 | ” | ” |
| 31375 | ” | ” | | 5.32 | 25.37 | 0.12683 | 0.511775±3 | 2212 | 1873 | 0.50993 | 2.12 | ” | ” |
| 9608 | metapyroxenite | ” | | 6.69 | 32.92 | 0.12283 | 0.511724±4 | 2200 | 1876 | 0.50994 | 0.93 | 1980 | ” |
| 43745 | amphibolite | ” | | 2.67 | 14.17 | 0.11407 | 0.511583±4 | 2222 | 1936 | 0.50991 | 2.77 | 2200 | ” |
| 18761 | metadiabase | ” | | 7.23 | 30 | 0.14575 | 0.511944±4 | 2460 | 2063 | 0.50959 | 0.93 | 2214 | ” |
| 67-4 | plagiogneiss | Garsjo | A | 1.08 | 6.93 | 0.09416 | 0.510755±2 | 2919 | 2779 | 0.50894 | 0.74 | 2840 | ” |
| 56-1 | ” | ” | B | 2.18 | 11.5 | 0.11486 | 0.511242±4 | 2778 | 2583 | 0.50914 | 2.68 | ” | ” |
| 65-1 | ” | ” | B | 6.41 | 38.97 | 0.09948 | 0.510934±3 | 2814 | 2654 | 0.50909 | 2.29 | ” | ” |
| 76-1 | ” | Varanger | B | 1.91 | 12.17 | 0.09494 | 0.510776±4 | 2911 | 2770 | 0.50895 | 0.86 | 2810 | ” |
| 111-1 | ” | Svanvik | A | 2.15 | 15.25 | 0.08521 | 0.510617±5 | 2877 | 2744 | 0.50900 | 1.32 | 2825 | ” |
| 109/99 | ” | ” | A | 2.34 | 9.85 | 0.1436 | 0.511703±6 | 2930 | 2663 | 0.508925 | 1.05 | ” | ” |
| 115/99 | ” | ” | A | 2.24 | 16.5 | 0.08199 | 0.510589±10 | 2838 | 2705 | 0.509053 | 1.73 | ” | ” |
| 55-8 | amphibolite | Garsjo | | 1.66 | 4.87 | 0.20591 | 0.512922±38 | | | 0.50638 | 2.15 | 2840 | ” |
| 65-9 | ” | ” | | 2.04 | 6.1 | 0.20272 | 0.512920±6 | | | 0.50313 | 3.29 | ” | ” |

Note: 5The $^{143}Nd/^{144}Nd$ value of the LaJolla standard was 0.512078±5 (n=10), this value for JiNd1 was 0.511833±6 (n = 11). T(DM) were calculated in compliance with the DePaolo (1981) model. No model ages of Samples 55-8 and 65-9 were calculated because of their elevated $^{147}Nd/^{144}Nd$ ratios, causing a manyfold increase in the T(DM) errors. *T, Ma, is the U–Pb and Rb–Sr age values (see text) assumed in the calculations of $\varepsilon_{Nd}$.

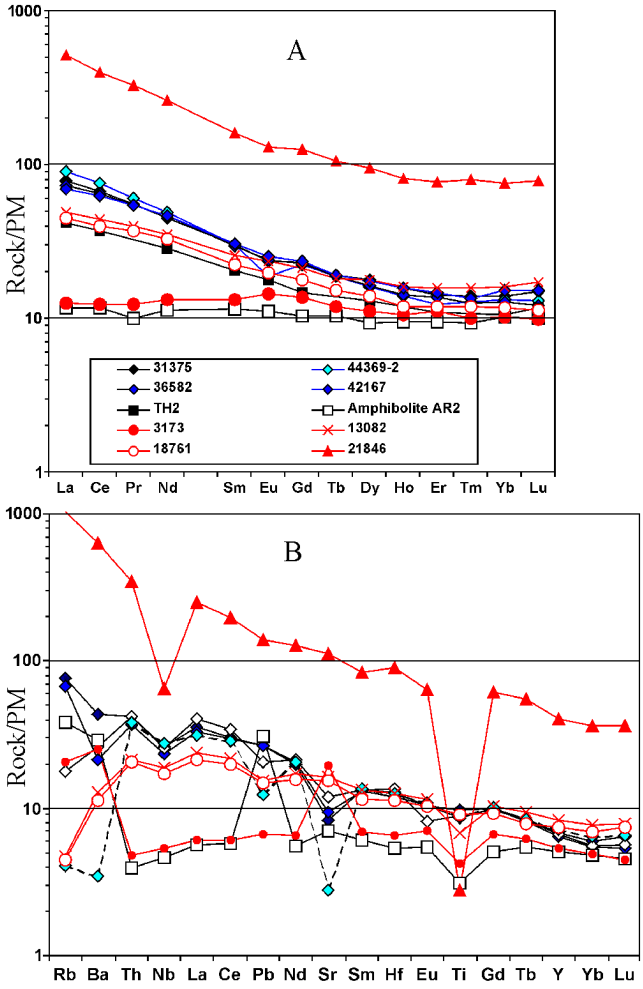


**Figure 6.** Concentrations of trace elements and REE in amphibolites of the dike facies (type I) from KSDB, normalized to (a) chondrite and (b) primitive mantle. TH2 – tholeiites of Archean greenstone belts [*Condie,* 1981]; amphibolite AR2 – average composition of amphibolites from the surroundings of KSDB. Samples 3173, 18761, 13082, and 21816 are basalts of the Matert, Zapolyarny, Kuetsjarvi, and Majarvi units of the Pechenga structure, respectively.

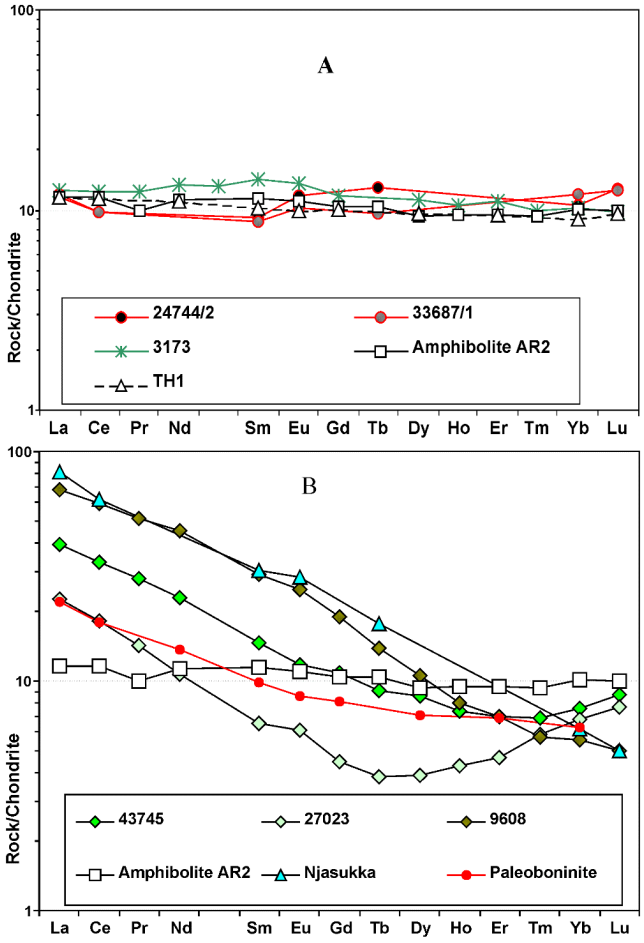


**Figure 7.** Chondrite-normalized REE patterns of (a) dike-facies amphibolites from KSDB (type II) and (b) KSDB metabasites. TH1 – tholeiites of Archean greenstone belts [*Condie,* 1981]. Data on the composition of rocks of the Nyasyukka Complex and paleoboninites are compiled from, respectively [*Smolkin et al.,* 1995] and [*Sharkov et al.,* 1997].

11.9), Zr, and Nb at elevated concentrations of Mg, Cr, and Ni. The amphibolites differ from the basalts of the Majarvi Formation of the Pechenga structure (which have a similar major-element composition) by lower concentrations of LREE, Ti, Ba, Sr, Zr, Cr, and Ni (Table 3, Figure 7a).

All amphibolites representing intrusive rocks in the KSDB Archean complex have REE concentrations and patterns notably different from those of the Archean amphibolites in the surroundings of KSDB (Tables 5, 8). Among these rocks, the highest LREE concentrations and the most fractionated REE patterns, with $(La/Yb)_n = 12.2$, are typical of metapyroxenites. As follows from Figure 7b, there is practically full coincidence between the REE patterns of these rocks and the pyroxenites of the Nyasyukka Complex [*Smolkin et al.,* 1995] in the northern framing of the Pechenga structure. The complex was dated at 1956±20 Ma by the Sm–Nd isochron technique [*Huhma et al.,* 1996]. The maximum estimates of the model age, $T_{Nd}(DM)$, of the studied metapyroxenite sample is 2200 Ma, which is consistent with its assignment to the Early Proterozoic.

The metagabbro (Samples 43745 and 27023) have major- and most trace-element concentrations analogous to those of the metadolerites and gabbronorites from dikes in the northern framing of the Pechenga structure (Table 5), which belong, according to Zh. A. Fedotov [*Smolkin et al.,* 1995], to picritodolerite and gabbronorite complexes dated at, respectively, 2200 and 2555 Ma. This correlation is confirmed by the Proterozoic model age of Sample 43745 (2222 Ma). It is also worth noting the elevated MgO contents of rocks in the samples examined (6.4–8.0% MgO) at $SiO_2$ contents of 53–51% and U-shaped REE patterns with a minimum at MREE and maxima over both LREE and HREE. These compositional features are inherent to the rocks of the

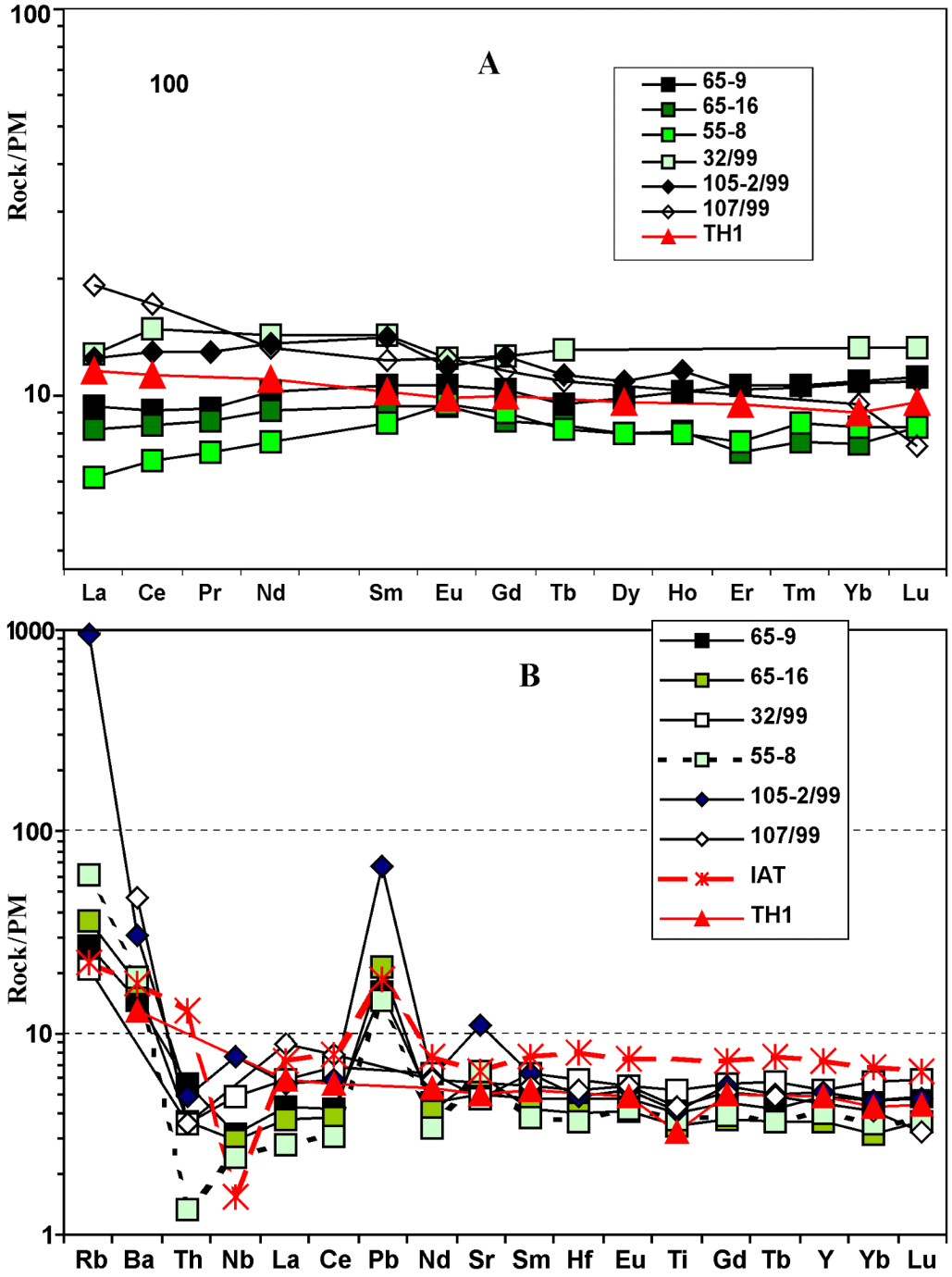


**Figure 8.** Concentrations of trace elements in amphibolites from the KSDB surroundings normalized to (a) chondrite and (b) primitive mantle. TH1 – tholeiites of Archean greenstone belts [*Condie,* 1981], IAT – tholeiitic basalts of the South Sandwich Islands [*Pearce et al.,* 1995].

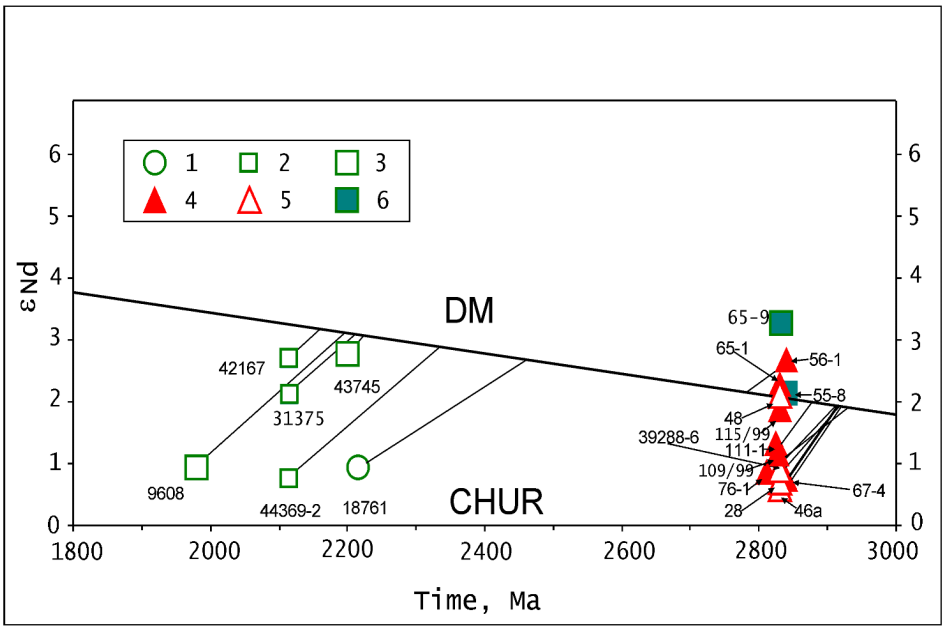


**Figure 9.** Diagram $\varepsilon_{Nd}$ vs. time for mafic rocks and tonalite–trondhjemite gneisses from KSDB and its surroundings.
(1) Trachybasalt; (2) mafic rocks of the dike facies; (3) mafic rocks of the intrusive facies (Sample 9608—metapyroxenite, Sample 43745—garnet–clinopyroxene gabbro); (4, 5) tonalite–trondhjemite gneisses from (4) the surroundings of KSDB and (5) KSDB; (6) amphibolite from KSDB surroundings. The Sm and Nd isotopic studies were carried out on a Finnigan MAT-262 mass spectrometer with the simultaneous registration of ion currents by all collectors. The $^{147}Sm/^{144}Nd$ ratios were measured accurate to ±0.3% ($2\sigma$), concentrations of elements were measured accurate to ±0.5% ($2\sigma$). DM and CHUR are the evolutionary lines of the $^{143}Nd/^{144}Nd$ ratio for the depleted mantle (DM) and chondritic uniform reservoir (CHUR).

marianite–boninite association typical of young island arcs [*Ewart et al.,* 1977]. In the Baltic Shield, ancient boninites are restricted mostly to the Sumian and Sariolian age levels [*Sharkov et al.,* 1997] but were also encountered among younger rocks of the Pechenga–Varzuga belt and its surroundings. Figure 7b presents the REE patterns of the studied metagabbro and paleoboninite samples from the Baltic Shield [*Sharkov et al.,* 1997], which show mostly similar configurations.

### Complexes Exposed at the Surface

*Biotite Plagiogneisses.* The chemistry of the Garsjø gneisses corresponds to that of tonalite and trondhjemite, and they range from quantitatively dominant aluminous (<15% $Al_2O_3$ at $SiO_2$ = 70%) to less abundant low-Al (<15% $Al_2O_3$) varieties with variable concentrations of REE. Based on REE pattrens, at least three types of these rocks can be recognized (Figure 10):

type A comprises rocks with strongly fractionated REE patterns, $(La/Yb)_n$ = 12–88, extremely depleted in HREE ($Yb_n$ = 1–3) and less strongly depleted in LREE ($La_n$ = 28–76);

type B is characterized by a moderate REE fractionation, $(La/Yb)_n$ = 20–32, with a deletion in HREE ($Yb_n$ = 3–5) and elevated concentrations of LREE ($La_n$ = 90–126);

type C has weakly fractionated REE patterns, $(La/Yb)_n$ = 7–28, is enriched in LREE ($La_n$ = 98–203) and HREE ($Yb_n$ = 7–13).

The first type includes meso- and leucocratic rock varieties with $Al_2O_3$ and CaO concentrations decreasing with increasing $SiO_2$ and without correlations of the Fe, Mg, and Ti with $SiO_2$. The irregular variations in the contents of Fe, Mg, Ti, HFSE, and HREE are controlled by variations in the amounts of mafic and accessory minerals, most probably, because of the primary heterogeneity in the textures and structures of the protolith. The rocks are characterized by varying concentrations of both LREE and HREE at clearly pronounced Eu maxima. Their distinctive features are high Sr concentrations and very low contents of HREE and Y, which are only comparable with or lower than those of typical Archean TTG. The elementary patterns of these rocks have steep slopes with an enrichment in LILE and LREE relative to HFSE at well pronounced negative anomalies of Nb, Ti, and P (Figures 10a, 11a), i.e., features typical of Archean grey gneisses [*Martin,* 1994].

Having similar $SiO_2$ contents, the plagiogneisses of type B are higher in Ti, Fe, HFSE, and HREE than the type-A gneisses (Figures 10b, 11b), that were resulted from higher concentrations of mafic and accessory minerals. The compositional differences between the gneiss types could not be due

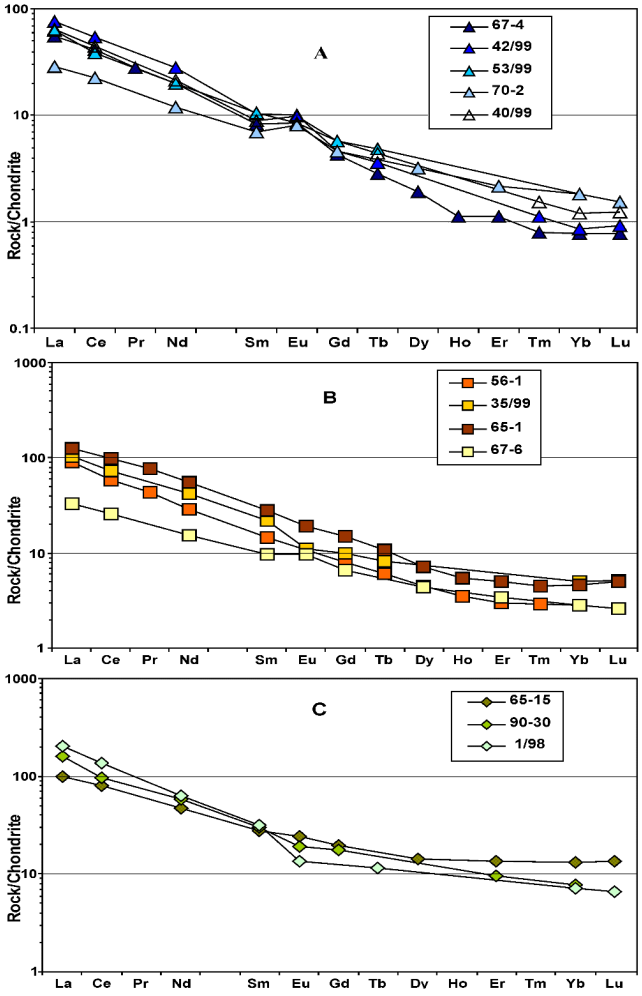


**Figure 10.** Chondrite-normalized REE patterns of tonalite–trondhjemite gneisses of the Garsjø Complex. A, B, and C are the geochemical types of gneisses.

to the fractional crystallization of a single parental magma or distinct partial melting degrees of the source, because, at similar $SiO_2$, $Al_2O_3$, and CaO concentrations, the gneisses differ in the concentrations of REE and HFSE. This led us to suggest that the rocks were generated under different $P-T$ conditions and/or were derived from distinct sources.

The low-Al gneisses of type C contain 66–70% $SiO_2$ and elevated concentrations of $TiO_2$, $Fe_2O_3$, REE, and HFSE but relatively low concentrations of Sr. The multi-element patterns of the type-C gneisses are characterized by gentler slopes than those of the gneisses of types A and B (Figures 10c, 11c). These compositional features of the rocks are generally atypical of Archean grey gneisses, which usually correspond to types A and B. At the same time, rocks of tonalite-trondhjemitic composition with weakly fractionated REE were identified among the TTG of the Superior Province in Canada [*Feng and Kerrich,* 1992], Amitsoq gneisses in Greenland [*Shimizu et al.,* 1998], in the Ancient Gneissic Complex of Swaziland [*Hunter et al.,* 1984], and in other shields.

The plagiogneisses of the Varanger Complex exhibit no clearly pronounced correlations between $SiO_2$ (68.1–71.4%)

**Table 5.** Concentrations of major and trace elements (wt % and ppm, respectively) in metagabbro (Samples 43745 and 27023) and metapyroxenite (Sample 9608) from KSDB in comparison with the composition of intrusive rocks exposed at the surface (Samples L315 and L415)

| Sample no. | 43745 | L315 | 27023 | L415 | 9608 |
|---|---|---|---|---|---|
| Depth, m | 11389 | | 7958 | | 9608 |
| $SiO_2$ | 53.03 | 52.09 | 51.13 | 49.56 | 46.56 |
| $TiO_2$ | 0.68 | 0.78 | 0.34 | 0.22 | 1.93 |
| $Al_2O_3$ | 14.68 | 14.65 | 18.74 | 18.12 | 7.56 |
| $Fe_2O_3$ | 10.69 | 10.85 | 8.76 | 8.1 | 15.53 |
| MnO | 0.17 | 0.19 | 0.15 | 0.16 | 0.22 |
| MgO | 6.38 | 6.86 | 7.97 | 8.06 | 13.81 |
| CaO | 10.34 | 9.81 | 9.52 | 9.06 | 9.9 |
| $Na_2O$ | 2.44 | 2.45 | 2.3 | 2.6 | 0.55 |
| $K_2O$ | 0.65 | 0.71 | 0.32 | 0.38 | 2.49 |
| $P_2O_5$ | 0.12 | 0.06 | 0.11 | 0.06 | 0.3 |
| LOI | 0.65 | 1.92 | 0.5 | 3.54 | 1.15 |
| Total | 99.83 | 100.37 | 99.84 | 99.86 | 100.00 |
| U | 0.48 | | 0.13 | | 0.59 |
| Th | 2.0 | | 1.0 | | 2.2 |
| Rb | 14 | 22 | 10 | 11 | 107 |
| Ba | 177 | | 75 | | 368 |
| Sr | 232 | | 335 | | 35 |
| La | 12.2 | | 7.1 | | 21.0 |
| Ce | 26.6 | | 14.8 | | 48.1 |
| Pr | 3.4 | | 1.7 | | 6.3 |
| Nd | 13.8 | | 6.4 | | 27.0 |
| Sm | 2.9 | | 1.3 | | 5.6 |
| Eu | 0.87 | | 0.45 | | 1.85 |
| Gd | 2.8 | | 1.2 | | 5.0 |
| Tb | 0.43 | | 0.18 | | 0.66 |
| Dy | 2.77 | | 1.26 | | 3.42 |
| Ho | 0.53 | | 0.31 | | 0.58 |
| Er | 1.48 | | 0.97 | | 1.47 |
| Tm | 0.23 | | 0.19 | | 0.18 |
| Yb | 1.58 | | 1.42 | | 1.16 |
| Lu | 0.28 | | 0.25 | | 0.16 |
| Zr | 81 | 100 | 46 | 38 | 160 |
| Hf | 2.0 | | 1.1 | | 4.1 |
| Ta | 0.21 | | 0.12 | | 1.44 |
| Nb | 2.8 | 9.0 | 1.8 | 5.0 | 20.2 |
| Y | 15.8 | 16.0 | 9.5 | 8.0 | 15.9 |
| Cr | 17 | 78 | 95 | 160 | 1047 |
| Ni | 116 | 150 | 204 | 270 | 645 |
| Co | 47 | 37 | 49 | 56 | 88 |
| V | 212 | 200 | 98 | 97 | 257 |
| Pb | 5.54 | | 6.11 | | 3.39 |
| $(La/Yb)_n$ | 5.2 | | 3.4 | | 12.2 |

Note: Analyses of Samples L315 and L415 are compiled from [*Smolkin et al.,* 1995].

**Table 6.** Concentrations of major and trace elements (wt % and ppm, respectively) in plagiogneisses of the Garsjø Complex

| Geoch. type | A | | | | | | B | | | C | | | |
|---|---|---|---|---|---|---|---|---|---|---|---|---|---|
| Sample no. | 67-4 | 67-6** | 42/99* | 53/99* | 70-2** | 40/99* | 56-1 | 35/99* | 65-1 | 65-15** | 91-170* | 90-30* | 1/98* |
| $SiO_2$ | 68.31 | 68.84 | 69.01 | 70.17 | 70.59 | 70.67 | 68.14 | 69.4 | 73.85 | 68.52 | 65.76 | 67.4 | 69.83 |
| $TiO_2$ | 0.18 | 0.41 | 0.177 | 0.392 | 0.47 | 0.316 | 0.41 | 0.502 | 0.44 | 0.77 | 0.68 | 0.62 | 0.42 |
| $Al_2O_3$ | 17.49 | 15.85 | 15.87 | 14.96 | 15.11 | 14.67 | 15.68 | 13.94 | 12.74 | 14.44 | 15.42 | 14.18 | 15.15 |
| $Fe_2O_3$ | 2.18 | 3.31 | 2.61 | 3.23 | 3.11 | 2.75 | 3.93 | 4.29 | 4.14 | 5.37 | 5.27 | 4.89 | 3.61 |
| MnO | – | 0.07 | 0.03 | 0.043 | 0.05 | 0.038 | 0.04 | 0.047 | – | 0.07 | 0.11 | 0.09 | 0.04 |
| MgO | 0.88 | 1.26 | 1.74 | 0.9 | 0.91 | 1.72 | 1.24 | 1.66 | 0.58 | 1.54 | 1.17 | 1.1 | 1.24 |
| CaO | 3.85 | 3.28 | 3.57 | 3.36 | 2.98 | 3.02 | 4.14 | 3.17 | 2.48 | 3.25 | 3.96 | 4.39 | 2.46 |
| $Na_2O$ | 5.1 | 4.14 | 4.9 | 5.12 | 4.48 | 4.89 | 3.99 | 4.61 | 3.83 | 3.24 | 4.64 | 3.93 | 4.55 |
| $K_2O$ | 1.48 | 1.39 | 1.15 | 1.25 | 1.2 | 1.37 | 1.43 | 1.68 | 1.30 | 1.88 | 1.43 | 0.99 | 1.68 |
| $P_2O_5$ | 0.1 | 0.11 | 0.03 | 0.104 | 0.07 | 0.033 | 0.13 | 0.081 | 0.08 | 0.13 | 0.18 | 0.12 | 0.08 |
| LOI | 0.28 | 1.11 | 0.6 | 0.57 | 0.57 | 0.14 | 0.7 | 0.7 | 0.39 | 0.89 | 0.44 | 0.41 | 0.69 |
| Total | 99.85 | 99.77 | 99.69 | 100.1 | 99.54 | 99.62 | 99.83 | 100.08 | 99.83 | 100.1 | 99.06 | 98.12 | 99.75 |
| U | 0.26 | | 0.4 | 0.5 | | 0.5 | 0.65 | 2.9 | 0.69 | | | | 1.2 |
| Th | 2.3 | | 3.0 | 6.6 | | 3.4 | 4.7 | 3.6 | 7.34 | | | | 5.1 |
| Rb | 41 | 106 | 32 | 79.5 | 69 | 52 | 57 | 94.9 | 74.52 | 96 | 79 | 36 | |
| Ba | 519 | | 350 | 270 | | 920 | 432 | 550 | 415.54 | | 332 | 227 | 100 |
| Sr | 547 | 344 | | 435 | 328 | | 345 | 388 | 153.51 | 275 | 269 | 263 | |
| La | 17.21 | 10.13 | 23.5 | 19.5 | 8.83 | 20 | 27.86 | 32 | 38.92 | 30.33 | 47.4 | 50 | 63 |
| Ce | 33.22 | 21.08 | 44 | 31 | 18.38 | 36 | 47.34 | 59 | 80.33 | 64.44 | 85.7 | 77.5 | 110 |
| Pr | 3.46 | | | | | | 5.26 | | 9.43 | | | | |
| Nd | 12.07 | 9.21 | 17.0 | 12 | 7.24 | 13 | 17.30 | 25 | 33.41 | 28.13 | 52.4 | 34.7 | 38 |
| Sm | 1.63 | 1.86 | 2.0 | 2.05 | 1.36 | 1.75 | 2.80 | 4.3 | 5.47 | 5.331 | 9.3 | 5.9 | 6.2 |
| Eu | 0.62 | 1.79 | 0.75 | 0.62 | 1.56 | 0.73 | 0.78 | 0.75 | 1.39 | 3.487 | 2.2 | 1.4 | 1 |
| Gd | 1.10 | 1.71 | 1.20 | 2.05 | 1.19 | 1.5 | 2.06 | 2.6 | 3.90 | 5.02 | 6.7 | 4.6 | 3.4 |
| Tb | 0.14 | | 0.17 | 0.23 | | 0.21 | 0.29 | 0.39 | 0.51 | | | | 0.54 |
| Dy | 0.61 | 1.42 | | | 1.02 | | 1.45 | | 2.32 | 4.563 | | | |
| Ho | 0.08 | | | | | | 0.25 | | 0.39 | | | | |
| Er | 0.23 | 0.72 | | | 0.45 | | 0.62 | | 1.06 | 2.808 | 3.6 | 2 | |
| Tm | 0.03 | | 0.036 | | | 0.05 | 0.09 | | 0.15 | | | | |
| Yb | 0.16 | 0.58 | 0.18 | 0.38 | 0.38 | 0.25 | 0.60 | 1.06 | 0.95 | 2.785 | 3.8 | 1.6 | 1.5 |
| Lu | 0.02 | 0.08 | 0.03 | 0.06 | 0.05 | 0.04 | 0.08 | 0.165 | 0.16 | 0.438 | | | 0.21 |
| Zr | 85 | 132 | | 225 | 191 | | 154 | 293 | 454.00 | 275 | 350 | 348 | |
| Hf | 2.4 | | 3.1 | 4.4 | | 5.5 | 3.68 | 6 | 10.68 | | | | 3.8 |
| Ta | 0.20 | | 0.17 | 0.27 | | 0.2 | 0.48 | 0.55 | 0.16 | | | | 0.5 |
| Nb | 3.2 | 9 | | 3.5 | <7 | | 5.0 | 7.9 | 5.22 | 10 | 22 | 7 | |
| Y | 2.3 | 6 | | 6 | <6 | | 7.4 | 11.8 | 10.74 | 22 | 36 | 22 | |
| Cr | 6.2 | 7.7 | 65 | 15.5 | 7 | 8.5 | 16 | 47 | – | 28 | 2 | 17 | 9 |
| Ni | 7.9 | 22 | | | 14 | | 13 | | 6.19 | 43 | 2 | 9 | |
| Co | 4.7 | <10 | 5.5 | 8.5 | 7 | 5.9 | 10 | 13.5 | 5.03 | 13 | 5 | 7 | 7.9 |
| V | 17 | 50 | | | 43 | | 50 | | 15.30 | 75 | 45 | 34 | |
| $(La/Yb)_n$ | 72.1 | 11.7 | 88.0 | 34.6 | 15.8 | 53.9 | 31.5 | 20.4 | 27.50 | 7.3 | 8.4 | 21.1 | 28.3 |
| $Eu/Eu^*$ | 1.34 | 3.02 | 1.37 | 0.92 | 3.67 | 1.35 | 0.95 | 0.64 | 0.87 | 2.03 | 0.81 | 0.79 | 0.61 |

and other major components but have a clear positive correlation between the LREE and Th concentrations (because of the simultaneous occurrence of these elements in accessory minerals). The gneisses are characterized by a fractionated REE patterns with $(La/Yb)_n$ = 11.6–40.1 at low concentrations of HREE ($Yb_n$ = 1.5–1.9, Figure 12a). The progressive depletion of the gneisses in LREE and MREE is coupled with an increase in the Eu maximum that relates with decrease in REE-bearing mineral contents, such as allanite, epidote, and apatite. It could reflect the fractionation of these minerals during the parental melt evolution. The most conspicuous features of these rocks are their high LREE, Rb, and Ba concentrations at low concentrations of HREE and pronounced Ta, P, and Ti minima (Figure 13), i.e., typical features of Archean grey gneisses.

The biotite gneisses of the main phase of the Svanvik Complex are characterized by all distinctive features of the high-Al trondhjemites: a strongly fractionated REE pat-

**Table 7.** Concentrations of major and trace elements (wt % and ppm, respectively) in plagiogneisses of the Varanger and Svanvik Complexes

| Complex | Varanger | | | | Svanvik | | | | | | |
|---|---|---|---|---|---|---|---|---|---|---|---|
| Geoch. type | A | | | | A | | | | B | | |
| no. | 76-1 | 70/99* | 59/99* | 69/99* | 109/99* | 112/99* | 115/99* | 111-1 | 113/99* | 108-2 | 106/99* |
| $SiO_2$ | 71.39 | 68.07 | 68.79 | 70.48 | 67.92 | 69.48 | 68.83 | 69.57 | 70.41 | 72.78 | 73.23 |
| $TiO_2$ | 0.25 | 0.345 | 0.354 | 0.29 | 0.353 | 0.312 | 0.354 | 0.26 | 0.225 | 0.21 | 0.117 |
| $Al_2O_3$ | 15.33 | 15.99 | 16.38 | 15.84 | 16.74 | 16.56 | 16.69 | 16.26 | 15.99 | 14.81 | 15.14 |
| $Fe_2O_3$ | 2.46 | 2.78 | 3.07 | 2.9 | 3.53 | 2.63 | 3.2 | 2.45 | 2.28 | 2 | 1.17 |
| MnO | – | 0.044 | 0.05 | 0.033 | 0.063 | 0.057 | 0.047 | – | 0.031 | – | 0.03 |
| MgO | 0.65 | 1.78 | 1.7 | 1.83 | 1.33 | 1.19 | 1.33 | 0.8 | 0.97 | 0.46 | 0.6 |
| CaO | 2.75 | 3.34 | 3.39 | 3.78 | 3.84 | 3.28 | 3.56 | 3.37 | 2.79 | 2.5 | 1.67 |
| $Na_2O$ | 4.5 | 6.15 | 4.36 | 4.01 | 3.51 | 4.74 | 3.73 | 4.87 | 4.14 | 4.47 | 6 |
| $K_2O$ | 1.99 | 1.38 | 1.35 | 0.54 | 1.14 | 1.26 | 1.55 | 1.38 | 1.58 | 2.01 | 0.92 |
| $P_2O_5$ | 0.12 | 0.03 | 0.065 | 0.05 | 0.104 | 0.092 | 0.099 | 0.12 | 0.065 | 0.08 | 0.041 |
| LOI | 0.37 | 0.22 | 0.22 | 0.02 | 0.74 | 0.55 | 0.7 | 0.74 | 0.7 | 0.51 | 0.64 |
| Total | 99.81 | 100.13 | 99.73 | 99.77 | 99.27 | 100.15 | 100.09 | 99.82 | 99.18 | 99.83 | 99.56 |
| U | 0.49 | 0.7 | 0.6 | 0.7 | 0.5 | 0.9 | 1.8 | 0.77 | 0.6 | 0.6 | 1.7 |
| Th | 5.7 | 1.3 | 0.5 | 0.8 | 1.5 | 3.6 | 2.5 | 3.9 | 1.9 | 3.5 | 3.3 |
| Rb | 85 | 63 | 67 | 10 | 67.5 | | 75.7 | 52 | 61.5 | 65.6 | 67.4 |
| Ba | 497 | 300 | 305 | 400 | 465 | 365 | 400 | 344 | 540 | 468 | 530 |
| Sr | 262 | | | | 807 | | 766 | 605 | 641 | 241 | 394 |
| La | 21.5 | 15.0 | 7.0 | 5.7 | 12 | 22 | 27.5 | 25.3 | 14.5 | 13.9 | 8.8 |
| Ce | 41.3 | 30.0 | 14.0 | 13.0 | 21 | 38 | 48 | 48.8 | 27 | 24.7 | 15 |
| Pr | 4.4 | | | | | | | 5.4 | | 2.6 | |
| Nd | 15.3 | 11.0 | 6.0 | 5.0 | 12 | 16 | 19 | 18.5 | 11 | 8.9 | 5.7 |
| Sm | 2.3 | 1.5 | 1.2 | 0.7 | 3 | 2.7 | 3.1 | 2.4 | 1.8 | 1.6 | 0.83 |
| Eu | 0.69 | 0.71 | 0.61 | 0.65 | 0.83 | 0.62 | 0.75 | 0.75 | 0.61 | 0.48 | 0.28 |
| Gd | 1.81 | 1.2 | 1.3 | 0.8 | 2.5 | 1.7 | 1.9 | 1.60 | 1.2 | 1.17 | 0.6 |
| Tb | 0.22 | 0.17 | 0.19 | 0.14 | 0.49 | 0.18 | 0.19 | 0.21 | 0.15 | 0.16 | 0.072 |
| Dy | 1.15 | | | | | | | 0.94 | | 0.74 | |
| Ho | 0.17 | | | | | | | 0.15 | | 0.11 | |
| Er | 0.47 | | | | | | | 0.38 | | 0.28 | |
| Tm | 0.05 | 0.06 | 0.06 | 0.06 | | | | 0.06 | | 0.04 | |
| Yb | 0.36 | 0.32 | 0.40 | 0.33 | 1.13 | 0.7 | 0.45 | 0.35 | 0.32 | 0.25 | 0.145 |
| Lu | 0.06 | 0.05 | 0.05 | 0.05 | 0.15 | 0.10 | 0.053 | 0.05 | 0.045 | 0.037 | 0.016 |
| Zr | 141 | | | | 98.4 | | 149 | 131 | 114 | 144 | 84 |
| Hf | 3.60 | 4.3 | 5.0 | 4.3 | 4.3 | 3.3 | 4 | 2.98 | 3.5 | 3.59 | 2.3 |
| Ta | 0.30 | 0.30 | 0.05 | 0.13 | 0.2 | | 0.35 | 0.34 | 0.17 | 0.32 | 0.29 |
| Nb | 4.3 | | | | 2.7 | | 2.75 | 3.3 | 3 | 3.4 | 2.3 |
| Y | 5.1 | | | | 12.9 | | 4.3 | 4.3 | 4.1 | 3.4 | 2.1 |
| Cr | 9 | 15 | 25 | 30.0 | 15.8 | 19.0 | 20.0 | 7 | 10.0 | 6.0 | 1.4 |
| Ni | 6 | | | | | | | 6 | | – | |
| Co | 5 | 7 | 7 | 6.2 | 9.5 | 6.2 | 8.5 | 5 | 6.2 | 4 | 4.2 |
| V | 24 | | | | | | | 25 | | 17 | |
| $(La/Yb)_n$ | 40.1 | 31.6 | 11.8 | 11.6 | 7.2 | 21.2 | 41.2 | 48.7 | 30.5 | 36.9 | 40.9 |
| $Eu/Eu^*$ | 1.00 | 1.57 | 1.49 | 2.65 | 0.90 | 0.83 | 0.88 | 1.10 | 1.20 | 1.04 | 1.16 |

terns and high Sr contents up to 800 ppm (Table 6, Figure 12b). The second-phase trondhjemites are more leucocratic (70.4–73.2% $SiO_2$) and are depleted in Al, Ca, Fe, Ti, Mg, LREE, and Sr compared with the first-phase gneisses (Figure 12c). These features confirm genetic relations between the rocks of the two phases of this complex and can be accounted for by the fractionation of amphibole, plagioclase, and allanite during crystallization of the parental melt.

*Gneisses with High-Al Minerals.* The $SiO_2$ concentrations of biotite and amphibole–biotite gneisses with muscovite, sillimanite, and garnet range from 52.3 to 70.5% (Table 2) and are negatively correlated with CaO, $Fe_2O_3$, $TiO_2$, and MgO at the absence of pronounced correlation with al-

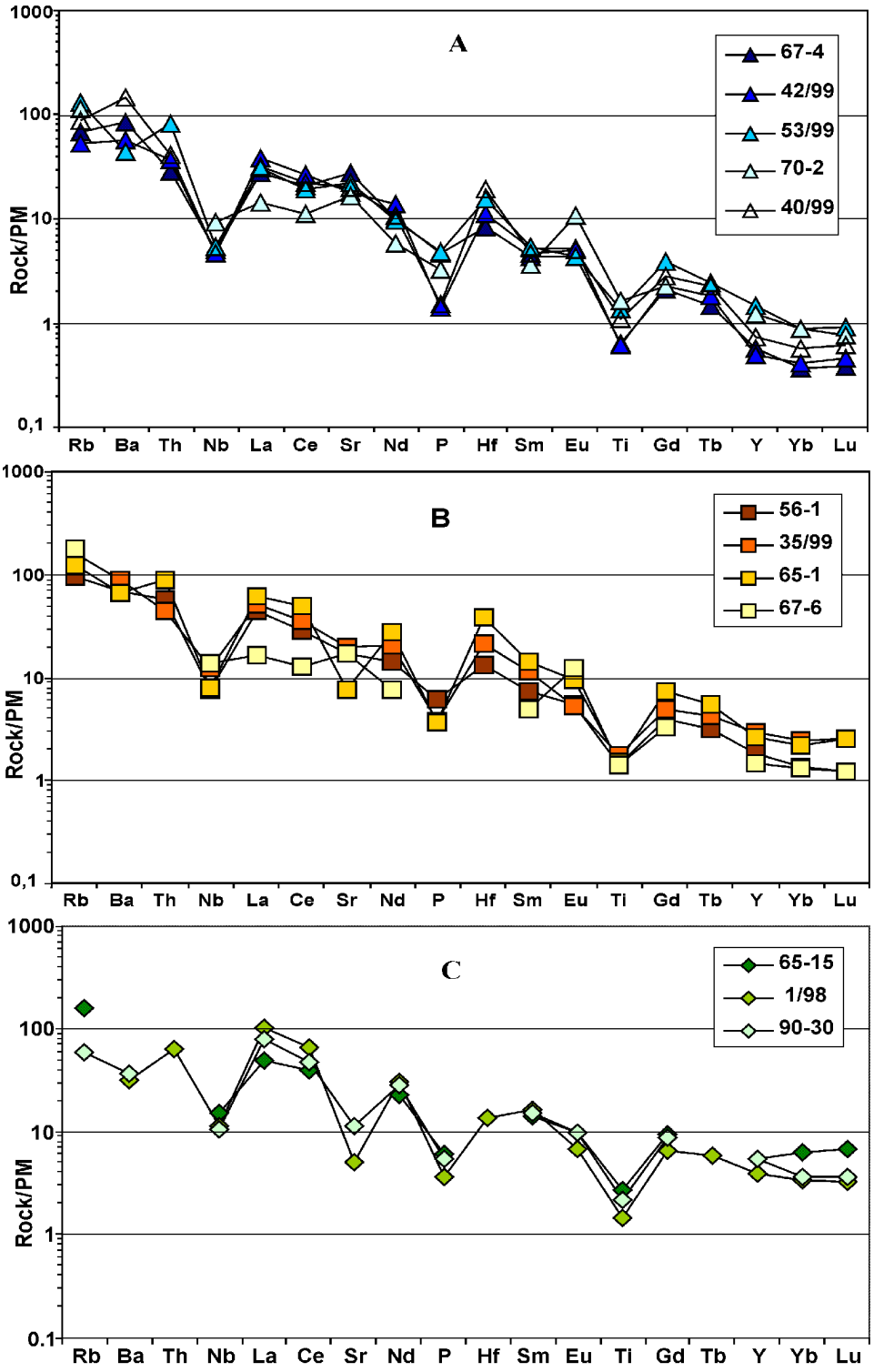


**Figure 11.** Concentrations of trace elements in tonalite–trondhjemite gneisses of the Garsjø Complex normalized to the primitive mantle. A, B, and C are the geochemical types of gneisses.

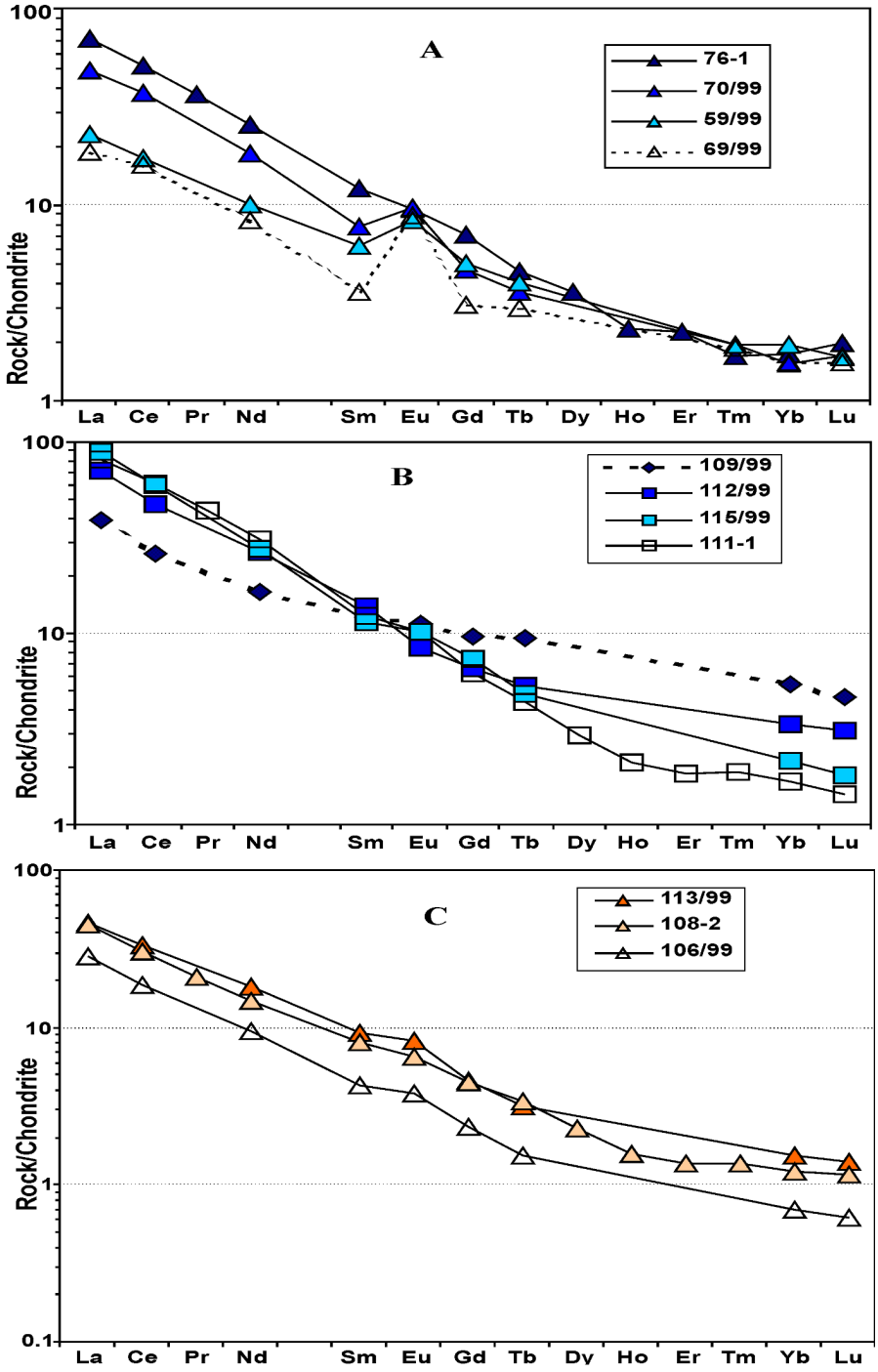


**Figure 12.** Chondrite-normalized REE patterns of tonalite–trondhjemite gneisses of (a) the Varanger Complex and (b and c) the first and second phases of the Svanvik Complex.

kalis, Rb, Ba, Sr, and REE. The gneisses have moderately fractionated REE patterns $(La/Yb)_n = 4.7–16.2$, Figure 14, which is similar to this parameter of Archean shales; [*Taylor and McLennan,* 1985]. The distinctive compositional features of the gneisses with HAM, such as regular variations in the least mobile major elements coupled with an uneven distribution of trace elements in rocks of variable silicity, suggest that the protoliths of the rocks could consist of weakly differentiated sediments ranged from argillite to sandstone. The various degrees of HREE depletion may be indicative of variable contributions of mafic rocks and TTG to these sediments.

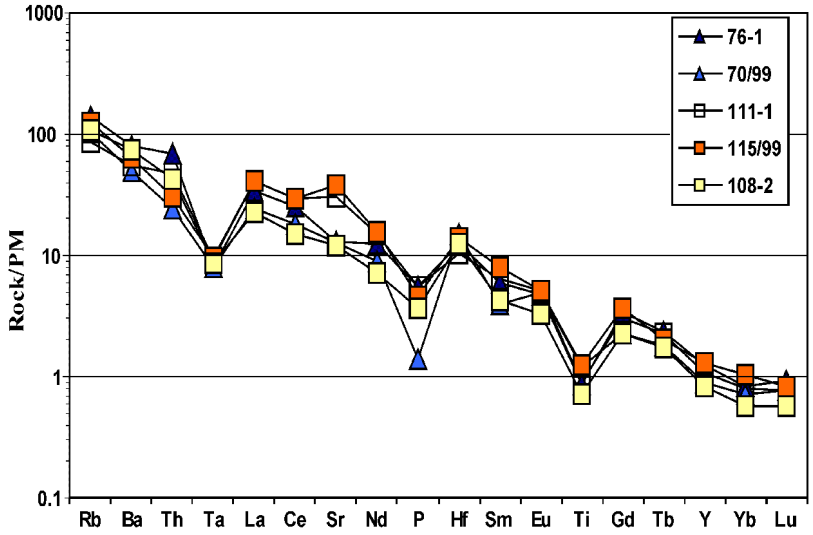


**Figure 13.** Concentrations of trace elements in tonalite–trondhjemite gneisses of the Varanger and Svanvik complexes normalized to the primitive mantle.

*Amphibolites.* In terms of normative composition, the amphibolites correspond mostly to olivine tholeiite and, less often, to alkaline basalt (Samples 65-16 and 32/99) or quartz tholeiite (Table 8, Sample 107/99). The amphibolites are characterized by relatively low concentrations of LREE and gently sloping REE patterns $(La/Yb)_n$ = 0.7–2.0. Except for most mobile elements (such as Rb, Ba, and Pb), the multi-element patterns of the rocks are quite flat, with small negative Ti anomalies (Figure 8). These features make the rocks sharply different from the Proterozoic amphibolites in the KSDB Archean complex but similar to TH1, the most widespread basalts of Archean greenstone belts [*Condie,* 1981], and to the modern subduction-related tholeiites [*Pearce et al.,* 1995]. Exceptions are amphibolites of Samples 107/99 and 105-2/99 from the Svanvik Complex, which are enriched in REE, Rb, Ba, Pb, and Sr, perhaps, because of their extensive migmatization (3.2–5.4% $K_2O$ and up to 51.3% $SiO_2$). In terms of Sm–Nd isotopic composition the mantle source of amphibolites from the Garsjø Complex was a depleted or strongly depleted ($\varepsilon_{Nd}$ = 2.15–3.3 for an age of 2.84 Ga (Table 4).

## Reconstruction of the Protolith Composition

Reconstruction of the genesis and composition of the protoliths provides valuable information for correlation between

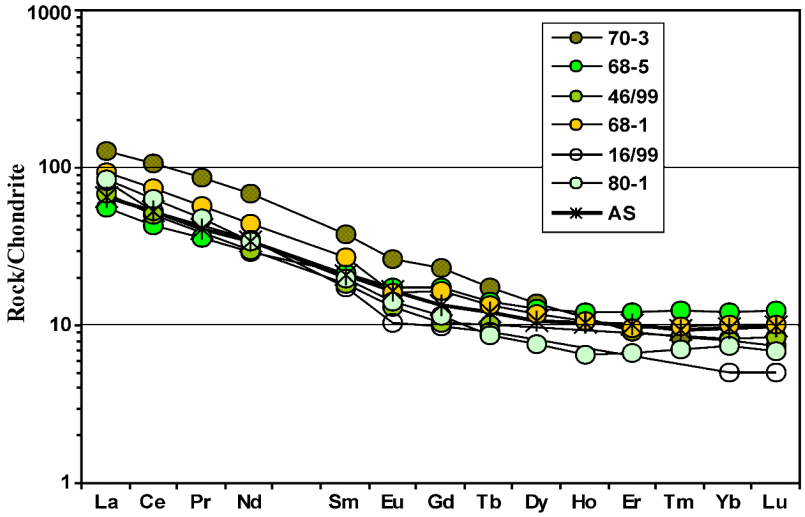


**Figure 14.** Chondrite-normalized REE patterns of gneisses with HAM from the Garsjø Complex. AS is the average Archean schist [*Taylor and McLennan,* 1985].

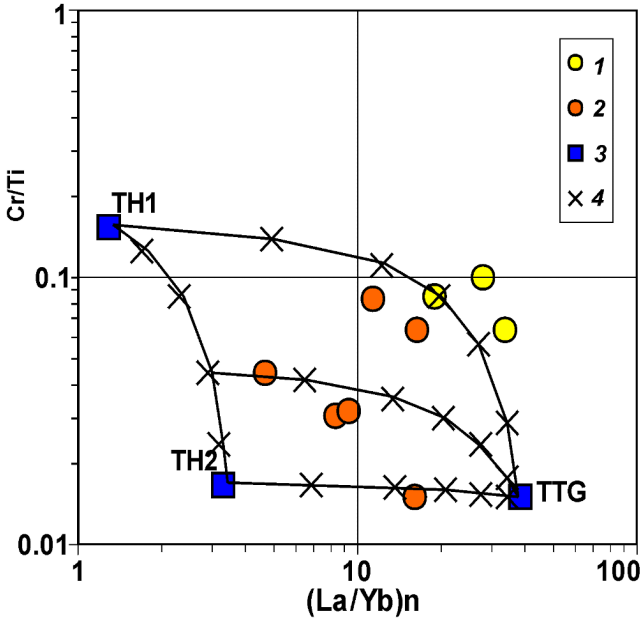


**Figure 15.** Cr/Ti vs. $(La/Yb)_n$ diagram for the composition of the source of gneisses with HAM. Compositions of TH1, TH2, and TTG are compiled from [*Condie,* 1981; *Martin,* 1994]. Vertical successions on the mixing lines correspond to 10, 30, 50, 70, 90, and 100% contribution of basalts of variable Mg#.

deep-seated rocks and their analogues exposed at the surface. The composition of the protoliths was identified based on the assumption of the isochemical character of metamorphism with respect to the least mobile elements: REE, HFSE, and some major elements (Al, Mg, and Ti).

### Gneisses with High-Al Minerals

The gneisses with HAM are pervasively enriched in Fe, Mg, Ti along with LREE and HFSE, perhaps, because of the concentration of these elements in the detrital and clay material of the initial sedimentary rocks. The negative correlation between LREE and $SiO_2$ suggest that the protoliths were produced at the active participation of weathering and sedimentary differentiation processes. The most informative elements of the gneisses with HAM are REE, HFSE and Th. The Garsjø HAM-bearing gneisses have narrow range of these elements and consequently correspond to moderately differentiated sediments ($Al_2O_3/SiO_2 = 0.2$–$0.32$), which are similar in this parameter to gneisses from the KSDB sequence ($Al_2O_3/SiO_2 = 0.16$–$0.44$). REE are least likely to be redistributed during sedimentary and subsequent diagenetic processes [*McLennan,* 1989], so we used these elements to interpret origin of the gneisses within the framework of the model for mixing of material from different sources (tholeiitic basalts and gneisses of tonalite-trondhjemitic composition) [*Taylor and McLennan,* 1985]. Our estimates point to a significant involvement of the TTG source at a smaller input of the material of high-Mg mafic rocks in the protoliths of the gneisses with HAM from the KSDB sequence as compared with their analogues exposed at the surface (Figure 15). This conclusion implies the significant contribution of local erosion sources to the composition of sediments in ancient granite–greenstone terranes. These areas contained rocks of various compositions in different quantitative proportions.

**Table 8.** Concentrations of major and trace elements (wt % and ppm, respectively) in amphibolites from KSDB surrounding complexes

| Complex | Garsjø | | | | Svanvik | |
|---|---|---|---|---|---|---|
| no. | 55-8 | 32/99* | 65-16 | 65-9 | 105-2/99 | 107/99* |
| $SiO_2$ | 47.53 | 47.74 | 48.19 | 49.66 | 47.88 | 51.28 |
| $TiO_2$ | 0.81 | 1.126 | 0.75 | 0.87 | 0.89 | 0.928 |
| $Al_2O_3$ | 15.25 | 13.67 | 14.84 | 13.7 | 14.03 | 14.93 |
| $Fe_2O_3$ | 13.32 | 14.76 | 12.94 | 14.79 | 12.16 | 10.44 |
| MnO | 0.21 | 0.219 | 0.22 | 0.23 | 0.23 | 0.21 |
| MgO | 8.13 | 6.28 | 7.29 | 6.14 | 6.17 | 5.94 |
| CaO | 10.1 | 9.97 | 10.72 | 10.48 | 7.97 | 9.78 |
| $Na_2O$ | 2.29 | 3.91 | 2.86 | 2.33 | 0.17 | 0.3 |
| $K_2O$ | 1.04 | 1.11 | 1.14 | 0.94 | 5.38 | 3.25 |
| $P_2O_5$ | 0.09 | 0.09 | 0.1 | 0.1 | 0.11 | 0.083 |
| LOI | 1.09 | 0.68 | 0.79 | 0.58 | 4.86 | 2.1 |
| Total | 99.86 | 99.56 | 99.84 | 99.82 | 99.85 | 99.24 |
| U | 0.13 | 0.2 | 0.36 | 0.77 | 0.60 | 0.6 |
| Th | 0.11 | 0.3 | 0.31 | 0.47 | 0.41 | 0.3 |
| Rb | 39 | 13 | 23 | 17 | 625 | |
| Ba | 134 | | 124 | 101 | 214 | 330 |
| Sr | 138 | 99 | 130 | 105 | 228 | |
| La | 1.9 | 4 | 2.5 | 2.9 | 3.9 | 6 |
| Ce | 5.5 | 12 | 6.8 | 7.4 | 10.5 | 14 |
| Pr | 0.9 | | 1.0 | 1.1 | 1.6 | |
| Nd | 4.6 | 8.6 | 5.5 | 6.1 | 8.2 | 8 |
| Sm | 1.7 | 2.8 | 1.8 | 2.1 | 2.7 | 2.4 |
| Eu | 0.70 | 0.92 | 0.69 | 0.79 | 0.88 | 0.92 |
| Gd | 2.35 | | 2.2 | 2.7 | 3.27 | |
| Tb | 0.39 | 0.62 | 0.40 | 0.45 | 0.54 | 0.52 |
| Dy | 2.59 | | 2.6 | 3.2 | 3.52 | |
| Ho | 0.57 | | 0.58 | 0.73 | 0.83 | |
| Er | 1.59 | | 1.5 | 2.2 | 2.19 | |
| Tm | 0.28 | | 0.25 | 0.34 | 0.34 | |
| Yb | 1.74 | 2.8 | 1.6 | 2.3 | 2.26 | 2 |
| Lu | 0.27 | 0.43 | 0.27 | 0.36 | 0.35 | 0.24 |
| Zr | 41 | 50.6 | 43 | 52 | 56 | – |
| Hf | 1.13 | 1.8 | 1.2 | 1.5 | 1.51 | 1.6 |
| Ta | 0.16 | 0.1 | 0.18 | 0.22 | 0.39 | 0.16 |
| Nb | 1.7 | 3.45 | 2.1 | 2.2 | 5.4 | |
| Y | 18.0 | 23.7 | 16.6 | 21.8 | 23.0 | |
| Cr | 221 | 133 | 212.2 | 52.7 | 166 | 130 |
| Ni | 163 | | 122.3 | 65.9 | 102 | |
| Co | 56 | 57 | 52.5 | 56.0 | 47 | 55 |
| V | 279 | | 242 | 292 | 270 | |
| Pb | 2.66 | | 3.98 | 2.96 | 12.41 | |
| $(La/Yb)_n$ | 0.7 | 0.96 | 1.1 | 0.9 | 1.2 | 2.0 |

If this is actually the case, the use of metasediments for the purposes of correlation seems to be hardly justified.

### Amphibolites

In order to identify the distinctive features of the source of the Proterozoic dike amphibolites and metavolcanic rocks of the Pechenga structure, one can use the approach proposed by *Kerrich and Wymen* [1997]. In multi-element plots normalized to the primitive mantle (Figure 6b), a line passing through the points of the most conservative elements (HREE, Ti, Hf, and Nb) has a negative slope. It indicates the enriched mantle source of the amphibolites and metabasalts of the Pirttijarvi and Zapolyarnyi formations of the Pechenga structure. Sm–Nd isotopic data shown that most of the KSDB amphibolites were derived from a source of composition intermediate between those of the depleted mantle and CHUR, supports this conclusion. The application of this prosedure [*Kerrich and Wymen,* 1997] to the Archean amphibolites (Figures 7a, 8) led us to conclude that the Archean mantle was more depleted, that, in turn, is consistent with analogous conclusions made on the basis of the Sm–Nd systematics. Of course, the Proterozoic age of the bulk of the amphibolites precludes reliable correlation between mafic rocks in the lower part of the KSDB succession with Archean amphibolites in the surroundings of the borehole.

### Tonalite–Trondhjemite Gneisses

Gneisses of tonalite-trondhjemitic composition dominated among the suites of deep-seated rocks and analogous rocks exposed at the surface differ in textures, structures, and composition. The magmatic genesis of the gneisses follow from the similarities between their compositions with those of modern volcanic rocks (adakites) and are generally consistent with experimental data on the origin of the parental melts from mafic sources. The textural and structural features of the tonalite–trondhjemite gneisses allow for their subdivision into volcanic and coeval (or younger) plutonic facies. The gneisses are characterized by broad variations in the concentrations of trace elements, which depended on the crystallization and melting conditions. In HREE contents, the rocks vary from strongly depleted to enriched types. The KSDB plagiogneisses can be subdivided into two geochemically contrasting types. One of them (type A) is strongly depleted in HREE and dominates in the succession penetrated by the borehole, while the rocks of the other type (type B) are enriched in these elements and were encountered only in the upper portion of the succession. The Garsjø tonalite–trondhjemite gneisses exposed at the surface were classified into three geochemical types, which mostly include depleted and moderately enriched varieties. The low-Al gneisses with elevated HREE concentrations are less abundant. The presence of distinct geochemical rock types among the tonalite–trondhjemite gneisses of KSDB and its surroundings makes them suitable for reconstructions of the protolith composition and for correlation purposes.

The origin conditions of the parental melts for gneisses belonging to discrete geochemical types may be constrained based on their Sm and Nd isotopic compositions. In an $\varepsilon_{Nd}$ vs. T diagram, the points of the gneisses define two discrete fields with different $\varepsilon_{Nd}$ values for the gneisses of types A and B (Figure 9, Table 4). The lower field comprises the points of gneisses with relatively low $\varepsilon_{Nd}$ (0.69–1.05 at an average of 0.80) with relatively high model ages (2911–2930 at an average of 2917 Ma), most of which fall into type A. The upper field includes composition points with $\varepsilon_{Nd}$ = 1.32–2.68 (average 2.02) and model ages of 2778–2877 (average 2825) Ma, most of which belong to type B. The Sm–Nd systematics of the rocks suggest the origin of the type-A gneisses by the melting of more ancient and less depleted source than those of the type-B gneisses, which had a relatively shot crustal residenbe age. The concept of different protoliths of the type-A and B gneisses is also confirmed by the distinct Sm/Nd ratios of the rocks (0.172 and 0.161, respectively), whose values are though to be preserved in granitoids produced by the melting of the same source material [*Faure,* 1986]. The $^{143}Nd/^{144}Nd$ ratios of the amphibolites (0.512920–0.512922) exceed this value of CHUR (0.512636) and provide evidence of the essentially restitic nature of the mantle source of these rocks.

The concentrations of trace elements in a melt are known to be controlled by the respective concentrations in the source, its melting degree, and the bulk partition coefficients of these trace elements between the melt and residue, whose values depend, first and foremost, on the mineralogical composition of the residue. Hence, it can be suggested that the differences in the REE compositions of the type-A and B gneisses were resulted from both the compositional differences between their sources and a lower melting degree of the source of the type-B gneisses. A less probable scenario is the enrichment of the protolith of the type-A gneisses in incompatible elements immediately before its melting, because in this case the melts derived became enriched in REE but retained isotopic signatures of the depleted source.

According to experimental studies [*Beard and Logfren,* 1991; *Rapp and Watson,* 1995; *Rapp et al.,* 1991; and others], the melts of tonalite-trondhjemitic composition most probable form by the partial melting of metabasic sources. An increase in the garnet and clinopyroxene in the residues in equilibrium with the partial melts and a decrease in the hornblende and plagioclase with increasing temperature and pressure result in progressive depletion of the melts in HREE and enrichment in Sr. To evaluate the $P-T$ conditions under which the melts were generated and the composition of the most probable residues, it is expedient to use an Yb–Eu diagram [*Turkina,* 2000], which shows variations in the boundary concentrations of REE in the model geochemical types of melts (Figure 16). As follows from this diagram, most points of the tonalite–trondhjemite rocks plot near the fields of initial or evolved melts, which are shifted toward lower Yb and Eu concentrations in response to fractionation of amphibole and plagioclase during a melt crystallization. The KSDB tonalite–trondhjemite gneisses are localized within the fields of the two recognized geochemical types of the rocks. The protoliths of the gneisses depleted in HREE are close to the composition of melts generated

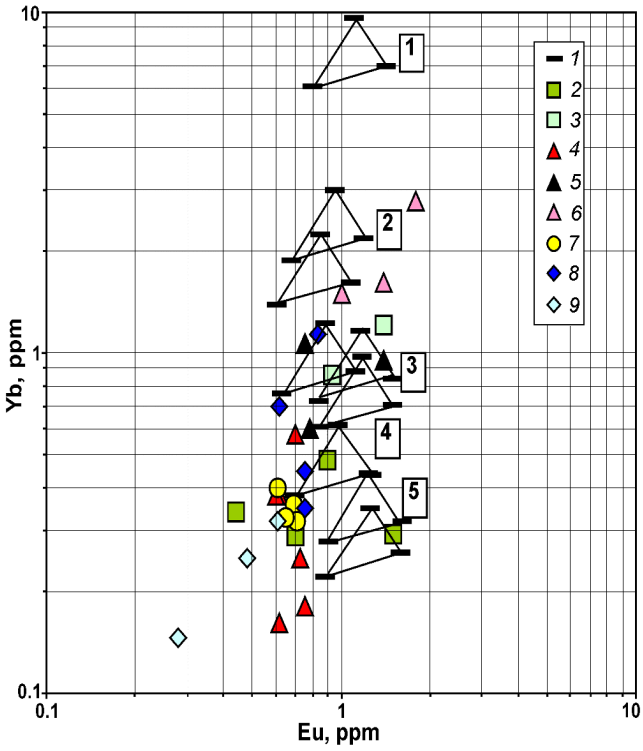


**Figure 16.** Yb vs. Eu diagram for tonalite–trondhjemite gneisses and model melts [*Turkina,* 2000]. (1) Model melts; (2, 3) tonalite–trondhjemite gneisses of types A and B from the succession penetrated by KSDB; (4–9) tonalite–trondhjemite gneisses of the Svanvik–Neiden segment: (4–6) gneisses of geochemical types A, B, and C of the Garsjø Complex, (7) gneisses of the Varanger Complex, (8) gneisses of the first and second phases of the Svanvik Complex. Triangles mark the compositional fields of melt derived by the dehydration melting of the sources of TH1, TH2, and NMORB in equilibrium with five types of residues (numbers in rectangles): (1) pyroxene–plagioclase, (2) plagioclase–amphibole±pyroxene, (3) garnet–plagioclase–pyroxene–amphibole (<20% garnet), (4) garnet–plagioclase–pyroxene–amphibole (>20% garnet), and (5) garnet–pyroxene.

in equilibrium with garnet-enriched amphibolite or eclogite residues at $P \geq 15-16$ kbar. Conversely, the protoliths of the gneisses enriched in HREE may have been derived under lower $P-T$, with the separation of garnet amphibolite residue. Similar melting conditions were also typical of the protoliths of the Garsjø tonalite–trondhjemite gneisses of types A and B. For type C most strongly enriched in HREE the partial melts could be derived only in equilibrium with garnet-free amphibolite residues corresponded to pressures of no more than 8 kbar. The tonalite–trondhjemite gneisses of the Varanger and Svanvik complexes are moderately depleted in HREE and generally belong to geochemical type A, whose protoliths were most probably formed in equilibrium with a garnet amphibolite residue, as also were the protoliths of ATTC in the lower part of the KSDB sequence. Hence, the analogy between the tonalite–trondhjemite gneisses penetrated by the borehole and those exposed at the surface is based not only on similarities in their compositions but also on the identity of their residual associations and the compositions of the metabasite sources.

## Processes of Proterozoic Magmatism and Metasomatism in the Basement Rocks of the Pechenga Structure

The most intense Proterozoic processes that affected the basement rocks of the Pechenga structure were the intrusion of numerous mafic–ultramafic bodies, retrograde metamorphism to medium- and low-temperature amphibolite and epidote amphibolite facies, intensive migmatization, and intrusions of 1.76-Ga postkinematic granites.

### Rocks of Mafic–Ultramafic Composition

As was demonstrated above, the inspected amphibolites from the lower part of the KSDB succession include rocks of Archean and Proterozoic ages, with the obvious predominance of the latter rocks (no less than 80% of the total amphibolite amount). The metabasalts of the dike facies seem to have served as magma conduits for the Pechenga volcanic rocks, while the amphibolites developing after the intrusive rocks are similar to the Proterozoic pyroxenites and paleoboninites from the framing of this structure. The mafic intrusive rocks in the Pechenga basement can be correlated with Proterozoic complexes of gabbroids, picrodolerites, Ti- and Fe-rich metadolerites, and metapicrites, which compose dike swarms in the framing rocks and have ages of, respectively, ~2555, 2200, and 1950 Ma. As follows from studies of paleorifts, the development of dike swarms of different ages is a characteristic feature of magmatism in these structures during different stages of their evolution [*Balagansky et al.,* 2001; *Bridgewater et al.,* 1995; *Kaz'min and Byakov,* 1997]. Similarly to the Pechenga metabasalts, it was proposed (based on Sm–Nd isotopic data) that the Proterozoic amphibolites were derived from a depleted mantle source, which was variably enriched in incompatible elements.

### Metamorphism and Migmatization

The Early Proterozoic retrograde metamorphism proceeded under low-temperature amphibolite, epidote amphibolite, and, seldom, greenschist facies conditions. G. G. Duk identified metamorphic zoning of the andalusite–sillimanite type produced during two metamorphic episodes: its high-temperature stages (of the amphibolite and epidote amphibolite facies) are coeval with the Luostari unit of the Pechenga Complex, and the higher temperature rocks correspond in age to the Nikel unit [*Duk et al.,* 1989]. The metamorphic processes of the amphibolite and epidote amphibolite facies were accompanied by migmatization of the

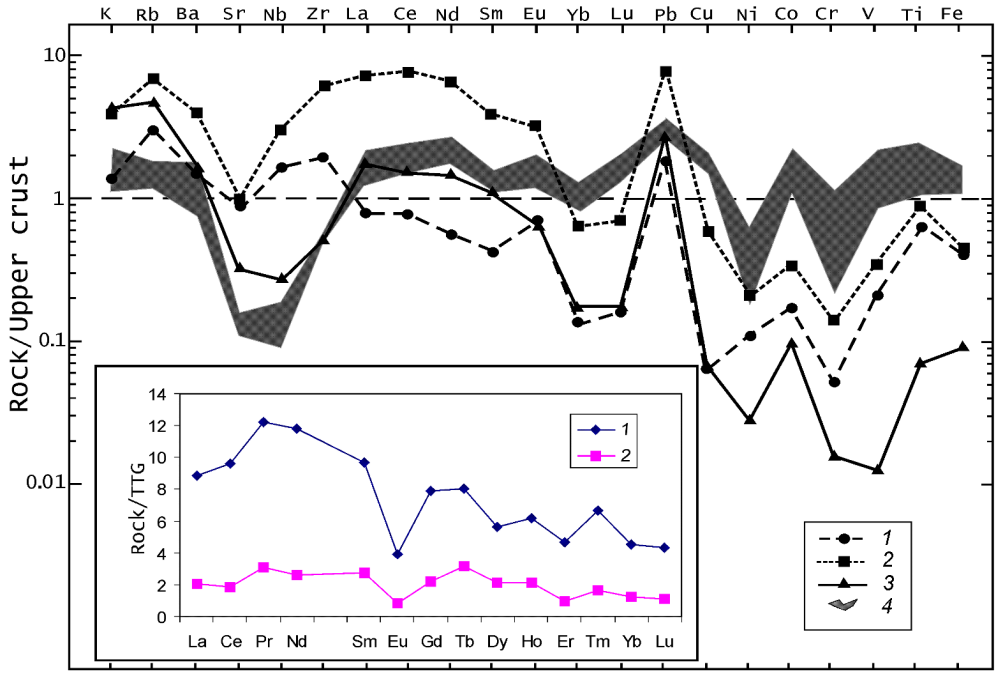


**Figure 17.** Average concentrations of major and trace elements in (1) tonalite–trondhjemite gneisses, (2) migmatized rocks of units 10 of KSDB, (3) metasomatic rocks in the northeastern framing of the Pechenga structure; (4) trachybasalts, basaltic andesites, trachybasaltic andesites, and andesites from the Kuetsjarvi unit of the Pechenga structure [*Kola Superdeep Borehole,* 1984, pp. 106–107], normalized to the concentrations of these elements in the continental crust [*Taylor and McLennan,* 1985]. The inset shows the REE concentrations of the migmatized rocks of (1) KSDB unit 10 and (2) metasomatic rocks from the northeastern framing of the Pechenga structure, normalized to tonalite–trondhjemite gneisses from KSDB.

rocks of the KSDB Archean complex. This process gave rise to a diversity of morphological types of migmatites. At the surface, analogous migmatites and granitic rocks compose a zone more than 20 km long and 2–6 km wide in the eastern framing of the Pechenga structure, which trends farther northwestward to the territory of Norway (Figure 1). The U–Pb zircon age of migmatized rocks in the lower part of the KSDB succession is 2225 Ma. The migmatization occurred locally, only beneath the Pechenga structure and its nearest surroundings, and was an apparently unequilibrated and allochemical process with respect to the host metamorphic rocks. It led to the depletion of the rocks in $Al_2O_3$, CaO, and $Na_2O$ and their enrichment in $SiO_2$, $TiO_2$, FeO, $K_2O$, and some trace elements (Rb, Ba, Nb, Zr, REE, Pb, Cu, Cr, Ni, Co V (Figure 17), F, P, and $CO_2$, which are typical of alkali-enriched rocks. In studying the isotopic composition of common Pb, it is commonly assumed that migmatization is triggered and maintained by fluids that segregated from a chamber of melts parental for the subalkaline volcanics of the Kuetsjarvi unit of the Pechenga Complex [*Vetrin et al.,* 2002a]. Fluid flows, directed from the crystallizing magma to the chamber roof, brought about migmatization of the upper crustal rocks through the precipitation of some major and trace elements from the fluids due to a decrease in solubilities of these elements in the fluids in response to a decrease in T and P. The same factors seem to have diminished the trace element concentrations in the rocks at the upper crustal levels as compared with he migmatized rocks in the lower parts of the succession and in the volcanics of the Kuetsjarvi unit, while the principal tendencies in the distribution of lithophile and siderophile elements remain similar (Figure 17). Data on the age of the KSDB migmatized rocks and "red granites" from the northeastern margin of the area led us to estimate the duration of the migmatization process at 50–70 m.y. [*Vetrin et al.,* 2000, 2002a].

## Postkinematic Granites

At depths of 9100–11,200 m, the Archean succession penetrated by KSDB was determined to contain numerous dikes of fine-grained, sometimes weakly porphyritic granites, which are analogous to the phase-4 granites of the Litza–Araguba Complex (LAC). The complex is exposed in the form of a chain of massifs in the eastern framing of the Pechenga structure. The concordant U–Pb zircon age of granite from depths of 9100–9700 m is 1765±2 Ma [*Kola Superdeep Borehole,* 1998]. A quite similar crystallization age value, 1762±9 Ma, was yielded by zircon from the LAC vein granite exposed at the surface [*Vetrin et al.,* 2000]. The initial $^4He/^3He$ ratio of He entrapped by the crystallizing granite was estimated at approximately $(3–5)\cdot10^5$ (Figure 18).

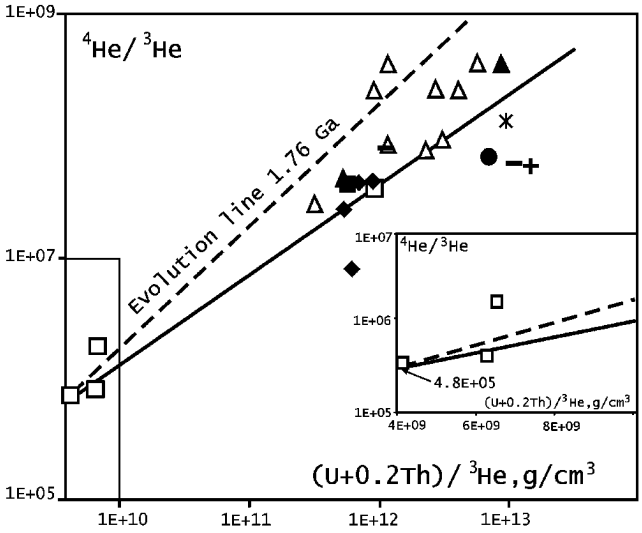


**Figure 18.** $^4He/^3He$ vs. (U + 0.2Th)/$^3$He diagram showing the proportions of parental and daughter isotopes in LAC rocks and minerals. The slope of the evolutionary line (dashed line) for an age of 1.76 Ga was calculated with allowance for the contribution of radiogenic He generated at given (U + 0.2Th) concentrations. The solid line is a regression whose intersection with the ordinate determines an initial ratio $^4He/^3He$ = 480,000. The inset shows a diagram (in linear coordinates) with data from the rectangle in the left-hand side of the diagram.

The genetic interpretation of the initial $^4He/^3He$ ratio was carried out within the framework of the mixing model of He from the continental crust and mantle. Based on studies of mantle xenoliths, the mantle source was assumed to be the enriched mantle of the area. Taking the values of the $^4He/^3He$ ratio in the enriched mantle and continental crust to be equal to, respectively, $6.7 \cdot 10^4$ and $1 \cdot 10^8$, we concluded that the values of $^4He/^3He = (3–5) \cdot 10^5$ of the granite could have been resulted from mixing of the mantle and crustal components in the proportion of approximately 1 to 4–7. These values indicate the essentially crustal nature of the entrapped fluid, which contained as little as ~13–22% mantle constituent [*Vetrin et al.,* 2002b]. The mantle–crustal model for the fluid genesis in granitoids is well compatible with the petrologic model for the genesis of these rocks mostly by the anatectic melting of the crust under the effect of mantle melts [*Vetrin et al.,* 1975].

## Conclusions

The basement of the Pechenga riftogenic structure, which was penetrated by the Kola Superdeep Borehole over a depth interval of 6842–12,261 m, is dominated by tonalite–trondhjemite gneisses, amphibolites, iron quartzites (jaspilites), and gneisses with aluminous minerals. Analogous rock associations are exposed at the surface as the Svanvik–Neiden segment in the northwestern part of the Kola–Norwegian block. The rocks of both the KSDB Archean complex and the Svanvik–Neiden segment have identical age and correspond to volcano-sedimentary and plutonic rocks typical of granite–greenstone terranes.

The geochemical features of the gneisses with HAM, such as high concentrations of LREE, HFSE, and mafic elements concentrated in the detritus and clay material along with the REE decreasing with increasing $SiO_2$, testify that the genesis of the protoliths involved the processes of weathering and sedimentary differentiation. The gneisses with HAM recovered by KSDB and sampled at the surface have similar, but not the same, sources. It was determined that local erosion sources contributed to the composition of the gneisses, and much material from high-Mg mafic rocks was involved in the gneisses with HAM from KSDB as compared with the analogous rocks exposed at the surface.

The great majority (≥80%) of amphibolites in the KSDB Archean complex are Early Proterozoic rocks of the dike facies, which seem to have formed magma feeders for the Pechenga volcanics. They were derived from a variably depleted mantle source with an insignificant input of material from an enriched mantle reservoir. The mafic intrusive rocks in the basement of the Pechenga structure can be correlated with the Proterozoic gabbronorite, picrodolerite, and Ti- and Fe-rich metadolerite and metapicrite complexes composing dike swarms in the framing of the structure and having ages of, respectively, ~2555, 2200, and 1950 Ma. The Late Archean amphibolites penetrated by KSDB and exposed at the surface have concentrations of major and trace elements close to those in TH1 basalts of Archean greenstone belts, fundamentally differ from Proterozoic amphibolites, and were derived from a depleted or strongly depleted mantle source.

Tonalite–trondhjemite gneisses dominate among the deep- and shallow-seated rocks of the granite–greenstone terrane and can be subdivided into plutonic and stratified volcanic facies, which include various genetic types. The variable composition of tonalite–trondhjemite gneisses make them convenient for correlating of rocks at different depths. The data obtained on the Sm–Nd isotopic systematics indicate that the protoliths of the REE-enriched gneisses (type B) have been derived from the depleted mantle-related metabasites ($\varepsilon_{Nd}$ = 1.05–2.68), whereas the source of the REE-depleted gneisses (type A) seem to have been less depleted in incompatible elements and radiogenic Nd ($\varepsilon_{Nd}$ = 0.58–1.73). The gneisses depleted in HREE were formed in equilibrium with residues of garnet-rich amphibolitic or eclogitic composition at least 15–16 kbar. The differences between the trace-element compositions of the gneisses belong to geochemical types A and B could be resulted from different source compositions and a lower melting degree of the type-B source. Conversely, the gneisses enriched in HREE may have been generated under lower pressures, with residues of garnet-free amphibolites.

Contrary to the associations exposed at the surface, the rocks of the KSDB Archean complex were extensively altered by Proterozoic magmatic and metasomatic processes related to the development of the Pechenga structure. The most active Proterozoic processes that affected the base-

ment of the structure were the intrusion of numerous mafic–ultramafic dikes, retrograde metamorphism to the medium-temperature amphibolite and epidote amphibolite facies, migmatization, and the emplacement of postkinematic granite intrusions at 1.76 Ga. Most Proterozoic processes show evidence of their relations with mantle sources. In general, the amounts of Proterozoic material introduced into the Archean rocks in the lower part of the borehole section plus the remobilized material of the Archean crust were evaluated at ≥30% (≥12–15% amphibolites, ∼3% vein granites, and ∼15% migmatized rocks).

**Acknowledgments.** The authors thank Yu. P. Smirnov, D. M. Guberman, and Yu. N. Yakovlev (of the Kola Superdeep Borehole Enterprise, Zapolyarnyi) for samples from the KSDB core provided for this research. O. Nordgulen (Geological Survey of Norway, Trondheim) is thanked for assistance in the organization and conduction of fieldworks at the territory of Norway. We appreciate valuable consultations with A. A. Kremenetsky (Institute of Mineralogy, Geochemistry, and Crystal Chemistry of Rare Elements, Moscow), V. F. Smolkin, and Yu. A. Balashov (Geological Institute, Kola Research Center, Russian Academy of Sciences, Apatity). The Sm–Nd isotopic geochemical study was carried out by A. A. Delenitzin and T. B. Bayanova; some samples taken at the surface in the surroundings of the borehole were analyzed for REE by V. A. Bobrov (United Institute of Geology, Geophysics, and Mineralogy, Siberian Branch, Russian Academy of Sciences, Novosibirsk). We are indebted to M. A. Vetrina for great help during the preparation of the manuscript. We thank Acad. F. P. Mitrofanov for continuous help and support in the organization of this research during all of its stages. This study was financially supported by the Russian Foundation for Basic Research, project no. 99-05-65158, and the IGCP-458 Project "Comparison of the Composition, Structure, and Physical Properties of Rocks and Minerals in the Kola Superdeep Borehole and Their Homologues on the Surface".

## References

*A seismological model for the lithosphere beneath Northern Europe: Lapland–Pechenga area,* Sharov, N. V., Ed. (in Russian), 226 p., Kol. Nauch. Tsentr, Russ. Akad. Nauk, Apatity, 1997.

*Archean complex in the section of the SG-3 borehole,* Mitrofanov, F. P., Ed. (in Russian), Kol. Nauch. Tsentr Russ. Akad. Nauk, Apatity, 1991.

Avakyan, K. Kh, *Geology and petrology of the Central Kola Archean granulite–gneiss terrane* (in Russian), Nauka, Moscow, 1982.

Balaganskii, V. V., V. M. Glaznev, and L. G. Osipenko, Early Proterozoic evolution of the northeastern Baltic Shield: terrane analysis (in Russian), *Geotektonika,* (2) 16–28, 1998.

Balagansky, V. V., M. J. Timmerman, N. Ye. Kozlova, and R. V. Kislitsyn, A 2.44 Ga syn-tectonic mafic dyke swarm in the Kolvitsa Belt, Kola Peninsula, Russia: implication for early Palaeoproterozoic tectonics in the north-eastern Fennoscandian Shield, *Precam. Res., 105,* 269–287, 2001.

Balashov, Yu. A., F. P. Mitrofanov, and V. V. Balagansky, New geochronological data on Archaean rocks of the Peninsula, Correlation of Precambrian formations of the Kola Karelian region and Finland, pp. 13–34, Apatity, 1992.

Balashov, Yu. A., and V. R. Vetrin, Reconstruction of the geodynamic environments of Archean magmatism and sedimentation, in *Archean complex in the sequence penetrated by SG-3,* Mitrofanov, F. P., Ed. (in Russian), Kol. Nauch. Tsentr Russ. Akad. Nauk, Apatity, 1991.

Barker, F., *Trondhjemites, dacites and related rocks,* Barker, F., Ed., Amsterdam: Elsevier, 1979.

Beard, J. S., and G. E. Lofgren, Dehydration melting and water-saturated melting of basaltic and andesitic greenstone and amphibolites at 1.3 and 6.9 kb, *J. Petrol., 32,* 465–501, 1991.

Bibikova, E. V., *U–Pb geochronology of the early evolutionary stages of ancient shields* (in Russian), Nauka, Moscow, 1989.

Bibikova, E. V., V. R. Vetrin, T. I. Kirnozova, V. A. Makarov, and P. Smirnov, Geochronology and correlations of rocks from the lower part of the KSDB sequence (in Russian), *Dokl. Russ. Akad. Nauk,* (332), 360–363, 1993.

Boynton, W. V., Cosmochemistry of the rare earth elements: meteorite studies, in *Rare earth element geochemistry,* Henderson, P. Ed., pp. 63–114, Elsevier, Amsterdam, 1984.

Bridgwater, D., F. Mengel, B. Fryer, P. Wagner, and S. C. Hansen, Early Proterozoic mafic dykes in the North Atlantic and Baltic cratons: field setting and chemistry of distinctive dyke swarms, in *Early Precambrian Processes. Geol. Society Spec. Publ.,* Coward, M. P. and Ries, A. C., Eds., (95) 193–210, 1995.

Chen, D., T. E. Krogh, V. R. Vetrin, and F. P. Mitrofanov, U–Pb geochronology of rocks from the Archean portion of the sequence penetrated by the Kola Superdeep Borehole, in *Kola Superdeep Borehole: Scientific results and research experience,* Orlov, V. P. and Laverov, N. P., Eds. (in Russian), pp. 59–70, Tekhnoneftegaz, Moscow, 1998.

Condie, K. C., *Archean Greenstone Belts,* Elsevier, Amsterdam, 1981.

DePaolo, D. J., Neodymium isotopes in the Colorado Front Range and mantle evolution in the Proterozoic, *Nature, 291,* 193–196, 1981.

Dobrzhinetskaya, L. F., O. Nordgulen, V. R. Vetrin, J. Cobbing, and B. A. Sturt, Correlation of the Archaean rocks between the Sorvaranger area, Norway, and the Kola Peninsula, Russia (Baltic Shield), *Geol. Unders., Spec. Publ., 7,* 7–28, 1995.

Dobrzhinetskaya, L. F., *Structural–metamorphic evolution of the Kola Group* (in Russian), Nauka, Moscow, 1978.

Duk, G. G., T. V. Kol'tsova, E. V. Bibikova, O. A. Levchenkov, I. M. Morozova, S. Z. Yakovleva, E. S. Bogomolov, A. M. Fedoseenko, and E. R. Drubetskoy, *Problems of deep-seated petrogenesis and age of rocks of the Kola Superdeep Borehole,* Levsky, L. K. and Levchenkov, O. A., Eds. (in Russian), pp. 72–86, Nauka, Leningrad, 1989.

Ewart, A., R. N. Brothers, and A. Mateen, An outline of the geology and geochemistry, and the possible petrogenetic evolution of the volcanic rocks of the Tonga–Kermadec–New Zealand island arc, *J. Volcanol., Geotherm. Res., 2,* (3) 205–250, 1977.

*Facies of regional metamorphism in the Kola Peninsula,* Goryainov, P. M., Ed. (in Russian), Nauka, Leningrad, 1977.

Faure, G., *Principles of isotope geology,* Wiley, New York, 1986.

Feng, R., and R. Kerrich, Geodynamic evolution of the southern Abitiby and Pontiac terranes: evidence from geochemistry of granitoid magma series (2700–2630 Ma), *Can. J. Earth Sci., 29,* 2266–2286, 1992.

Guberman, D. M., P. Smirnov, and S. V. Semashko, Continental crustal thickening in the geotravers of the Kola Superdeep Borehole (in Russian), *Razv. Okhr. Nedr,* (3) 10–11, 1994.

Huhma, H., V. F. Smolkin, E. J. Hanski, and Z. A. Fedotov, Sm–Nd isotope study of the Nyasyukka dyke complex in the northern Pechenga area, Kola Peninsula, Russia. Program and Abstracts, *IGCP Project 336 Symposium in Rovaniemi,* pp. 57–58, University of Turku Publ., 1996.

Hunter, D. R., F. Barker, and H. T. Millard, Geochemical investigation of Archaean bimodal and Dwalile metamorphic suites, Ancient Gneissic Complex, Swaziland, *Precambrian Res., 24,* 131–155, 1984.

Juve, G., L. Storseth, V. Vetrin, and L. P. Nilssen, Mineral deposits of the international 1: 250 000 Map-sheet Kirkenes, *Nor. Geol. Unders. Special Publ., 7,* 375–378, 1995.

Kaz'min, V. G., and A. F. Byakov, Continental rifts: structural control and continental breakup (in Russian), *Geotektonika,* (1) 20–31, 1997.

Kerrich, R., and D. A. Wyman, Review of developments in trace-element fingerprinting of geodynamic settings and their implications for mineral exploration, *Austral. J. Earth Sci., 44,* 465–487, 1997.

Kesola, R., Taka-Lapin metavulkaniitit ja niiden geologinen ymparisto, Lapin vulkaniittiprojektin raportti, *Espoo. Geol. Survey of Finland, 107,* 1991.

*Kola Superdeep Borehole: inspection of deep-seated structures in the continental crust with the aim of the Kola Superdeep Borehole,* Kozlovskii, E. A. Ed. (in Russian), Nedra, Moscow, 1984.

*Kola Superdeep Borehole: Scientific results and research experience,* Orlov, V. P. and Laverov, N. P., Eds. (in Russian), Tekhnoneftegaz, Moscow, 1998.

Kozlov, N. E., A. A. Avedisyan, A. A. Ivanov, et al., *Homologues of metamorphic rocks from the lower part of the Archean sequence penetrated by the Kola SG-3 superdeep hole (unit IX at depths of 11,411–11,708 m) and in exposures of the Zatuloma structure of the Kola–Norwegian domain* (in Russian), Izd. Murmansk Gos. Univ., Murmansk, 2001.

Kremenetsky, A. A., and L. N. Ovchinnikov, *Geochemistry of deep-seated rocks* (in Russian), Nauka, Moscow, 1986.

Levchenkov, O. A., L. K. Levsky, O. Nordgulen, L. F. Dobrzhinetskaya, V. R. Vetrin, J. Cobbing, L. P. Nilsson, and B. A. Sturt, U–Pb zircon ages from Sorvaranger, Norway and the western part of the Kola Peninsula, Russia, *Nor. Geol. Unders. Special. Publ., 7,* 29–48, 1995.

*Magmatic and metamorphic rock complexes of the Kola Superdeep Borehole* (in Russian), Kozlovsky, E. A., Ed., Nauka, Leningrad, 1986.

Martin, H., The Archean grey gneisses and the genesis of continental crust, in *Archean Crustal Evolution,* Condie, K. C., Ed., pp. 205–259, Elsevier, Amsterdam, 1994.

McLennan, S. M., Rare earth elements in sedimentary rocks: influence of provenance and sedimentary processes, *Rev. Mineral., 21,* 169–200, 1989.

Nordgulen, O., V. R. Vetrin, L. F. Dobrzhinetskaya, J. Cobbing, and B. Sturt, Aspects of late Archaean magmatism in the Sorvaranger–Kola terrane, northern Baltic Shield, *Nor. Geol. Unders., Spec. Publ., 7,* 49–63, 1995.

Pearce, J. A., and D. W. Peate, Tectonic implications of the composition of volcanic arc magmas, *Ann. Rev. Earth Planet. Sci., 23,* 251–285, 1995.

Pozhilenko, V. I., T. B. Bayanova, V. A. Bogachev, O. V. Gogol, O. A. Koshcheev, de K. Jong, M. J. Timmerman, and J. S. Daly, Refinement of the geotectonic nature and age of Early Precambrian processes and rocks based on isotopic data: a case study of the Kola Peninsula, Baltic Shield, *Thes. I Ross. conf on isotopic geochronology and isotopic dating of geologic processes: new techniques and results* (in Russian), pp. 268–271, Inst. Reol. Rudn. Mestor., Petrogr., Geokhim., Mineral., Russ. Akad. Nauk., Moscow, 2000.

Radchenko, A. T., V. V. Balaganskii, A. A. Basalaev, O. A. Belyaev, V. I. Pozhilenko, and M. K. Radchenko, *Explanatory notes to the geological map of the northeastern Baltic Shield. Scale 1 : 500 000* (in Russian), Kol. Nauch. Tsentr, Russ. Akad. Nauk, Apatity, 1994.

Rapp, R. P., and E. B. Watson, Dehydration melting of metabasalt at 8–32 kbar: implications for continental growth and crustal-mantle recycling, *J. Petrol., 36,* 891–931, 1995.

Rapp, R. P., E. B. Watson, and C. F. Miller, Partial melting of amphibolite/eclogite and the origin of Archeaen trondhjemites and tonalites, *Precam. Res., 51,* 1–25, 1991.

Sharkov, E. V., V. F. Smolkin, and I. S. Krasivskaya, The Early Proterozoic magmatic province of magnesian boninitic rocks in the eastern part of the Baltic Shield (in Russian), *Petrologiya, 5,* 503–522, 1997.

Shimizu, H., S. Nakai, S. Tasaki, A. Masuda, D. Bridgwater, A. P. Nutman, and H. Baadsgaard, Geochemistry of Ce and Nd isotopes and REE abundances in the Amitsoq gneisses, West Greenland, *Earth Planet. Sci. Lett., 91,* 159–169, 1988.

Siedletska, A., A. G. Krill, M. Often, J. S. Sandstad, A. Solli, E. Iversen, and B. Lieungh, Lithostratigraphy and correlation of the Archaean and Early Proterozoic rocks of Finnmarksvidda and the Sorvaranger district, *Nor. Geol. Unders., Bull., 403,* 7–36, 1985.

Smolkin, V. F., V. V. Borisova, S. A. Svetov, and A. E. Borisov, Late Archean komatiites of the Uraguba–Titovskaya structure in the northwestern Kola Peninsula (in Russian), *Petrologiya, 8,* (2), 199–224, 2000.

Smolkin, V. F., F. P. Mitrofanov, A. A. Avedisyan, et al., *Magmatism, sedimentogenesis, and geodynamics of the Pechenga paleorift structure* (in Russian), Kol. Nauch. Tsentr, Russ. Akad. Nauk, Apatity, 1995.

Sun, S.-S., and W. F. McDonough, Chemical and isotopic systematics of oceanic basalts: implications for mantle composition and processes, in *Magmatism in the Ocean Basins,* Saunders, A. D. and Norrys, M. J., Eds., Geological Society Spec. Publ., Oxford, 42, 313–345, 1989.

Taylor, S. R., and S. M. McLennan, *The continental crust: its evolution and composition,* Blackwell, London, 1985.

Timmerman, M. J., and J. S. Daly, Sm–Nd evidence for Late Archaean crust formation in the Lapland–Kola mobile belt, Kola Peninsula, Russia and Norway, *Precam. Res. 72,* 97–107, 1995.

Ts'on', O. V., M. V. Mints, P. G. Kostyuchenko, and S. G. Lapshin, Ages, geochemical features, and genesis of granitoids in the framing of the Pechenga volcano-tectonic depression (in Russian), *Geokhimiya, 7,* 1012–1018, 1988.

Turkina, O. M., Modeling geochemical types of tonalite–trondhjemite melts and their natural equivalents, *Geochem. Int.,* (7), 640–651, 2000.

Vetrin, V. R., A. N. Vinogradov, and G. V. Vinogradova, Petrology and facies–formation analysis of the Litza–Araguba diorite–granite complex, in *Intrusive charnockites and porphyritic granites of the Kola Peninsula* (in Russian), Batieva, I. D., Ed., pp. 149–316, Kol. Nauch. Tsentr Russ. Akad. Nauk, Apatity, 1975.

Vetrin, V., O. Nordgulen, J. Cobbing, B. Sturt, and L. Dobrzhinetskaya, The pyroxene-bearing tonalite–granodiorite–monzonite series of the northern Baltic Shield: correlation and petrology, *Nor. Geol. Unders. Spec. Publ., 7,* 65–74, 1995.

Vetrin, V. R., O. M. Turkina, and O. Nordgulen, Surface analogues of "grey gneiss" among the Archaean rocks in the Kola Superdeep Borehole (experience from petrologic-geochemical modelling of lower crust composition and conditions of formation of tonalite–trondhjemite rocks), Kola Science Centre Russ. Akad. Nauk, Apatity, 1999.

Vetrin, V. R., I. L. Kamensky, T. B. Bayanova, and S. V. Ikorsky, A mantle component in granitoids of the Litza–Araguba Complex at the surface and in the section of the Kola Superdeep Borehole: He isotopes in rocks and minerals, in *Data on the deep-seated rocks and physical processes in the section of the Kola Superdeep Borehole to a depth of 12,261 m* (in Russian), Mitrofanov, F. P., Ed., pp. 5–8, Kol. Nauch. Tsentr Russ. Akad. Nauk, Apatity, 2000.

Vetrin, V. R., I. L. Kemensky, and S. V. Ikorsky, Mantle fluid in Proterozoic granitoids: He and Ar isotopes in rocks and minerals of Litza–Araguba diorite–granite complex, Kola Peninsula (in Russian), *Petrologiya, 3,* 2002a (in press).

Vetrin, V. R., G. V. Ovchinnikova, L. A. Neymark, and B. V. Gorokhovsky, Migmatization of rocks of the Kola Superdeep Borehole Archean complex: age and sources of material, *Petrologiya, 2,* 2002b (in press).

Vinogradov, A. N., Metasomatic rocks associated with faults, in *Granitoid associations in the northeastern Baltic Shield* (in Russian), Bel'kov, I. ., Ed., pp. 80–95, Nauka, Leningrad, 1978.

Vinogradov, A. N., and G. V. Vinogradova, *Metamorphism of rocks of the Kola Group and assessment of the mica-mineralization potential of the northwestern Murmansk Province* (in Russian), pp. 19–30, Kol. Nauch. Tsentr Akad. Nauk SSSR, Apatity, 1973.

Vinogradova, N. P., A. S. Egorov, Yu. P. Smirnov, and V. P. Lyutoev, Tectonics of the Archean basement of the Pechenga riftogenic structure: evidence from the Kola Superdeep Borehole,

*Dokl. Russ. Akad. Nauk, 374,* (3) 362–365, 2000.

Yakovlev, N., T. B. Bayanova, D. M. Guberman, F. P. Mitrofanov, A. D. Pisarnitsky, and A. K. Yakovleva, Geological–geochronological subdivision of the Archean complex penetrated by the Kola Superdeep Borehole, in *III All-Russia conf "General problems of the subdivision of Precambrian"* (in Russian), pp. 284–287, Apatity, 2000.

Yakovleva, A. K., Mafic silicates, in *Arhcean complex in the section of the SG-3 superdeep borehole* (in Russian), Mitrofanov, F. P., Ed., pp. 61–117, Kol. Nauch. Tsentr, Russ. Akad. Nauk, Apatity, 1991.

Zagorodny, V. G., A. A. Predovsky, A. A. Basalaev, et al., *The Imandra–Varzuga zone of Karelides* (in Russian), Nauka, Leningrad, 1982.

(Received 18 March 2002)